HHS Public Access

Author manuscript

Eur J Inorg Chem. Author manuscript; available in PMC 2016 May 10.

Published in final edited form as:

Eur J Inorg Chem. 2015 May ; 2015(13): 2295–2307. doi:10.1002/ejic.201500097.

Hydrogen bonding and anticancer properties of water-soluble chiral *p*-cymene Ru(II) compounds with amino-oxime ligands

Yosra Benabdelouahab[a], **Laura Muñoz-Moreno**[b], **Malgorzata Frik**[c,d], **Isabel de la Cueva-Alique**[a], **Mohammed Amin El Amrani**[e], **María Contel**[c,d], **Ana M. Bajo**[b], **Tomás Cuenca**[a], and **Eva Royo**[a]

Eva Royo: eva.royo@uah.es

[a]Departamento de Química Orgánica y Química Inorgánica, Facultad de Química, Biología y Ciencias Ambientales, Universidad de Alcalá, 28871 Alcalá de Henares, Madrid, Spain

[b]Department of Systems Biology, Faculty of Medicine and Health Sciences, Universidad de Alcalá, 28871 Alcalá de Henares, Madrid, Spain

[c]Department of Chemistry, Brooklyn College, The City University of New York, Brooklyn, New York, 11210, United States

[d]Chemistry PhD Program, The Graduate Center, The City University of New York, 365 Fifth Avenue, New York, NY 10016, United States

[e]Université Abdelmalek Essaâdi, Faculté des Sciences, Departement de Chimie- Laboratoire de Chimie Organique Appliquée. Mhannech II, B.P : 2121 Tétouan, Morocco

Abstract

The investigation of the hydrogen-bonding effect on the aggregation tendency of ruthenium compounds [(η^6-*p*-cymene)Ru(κNHR,κNOH)Cl]Cl (R = Ph (**1a**), Bn (**1b**)) and [(η^6-*p*-cymene)Ru(κ^2NH(2-*pic*),κNOH)][PF_6]$_2$ (**1c**), [(η^6-*p*-cymene)Ru(κNHBn,κNO)Cl] (**2b**) and [(η^6-*p*-cymene)Ru(κNBn,κ^2NO)] (**3b**), has been performed by means of concentration dependence ^{1}H NMR chemical shifts and DOSY experiments. The synthesis and full characterization of new compounds **1c**, [(η^6-*p*-cymene)Ru(κNPh,κ^2NO)] (**3a**) and **3b** are also reported. The effect of the water soluble ruthenium complexes **1a-1c** on cytotoxicity, cell adhesion and cell migration of the androgen-independent prostate cancer PC3 cells have been assessed by MTT, adhesion to type-I-collagen and recovery of monolayer wounds assays, respectively. Interactions of **1a-1c** with DNA and human serum albumin have also been studied. Altogether, the properties reported herein suggest that ruthenium compounds **1a-1c** have considerable potential as anticancer agents against advanced prostate cancer.

Keywords

arene ruthenium compounds; oxime; chiral syntheses; non-covalent interactions; anticancer

Correspondence to: Eva Royo, eva.royo@uah.es.

Supporting information for this article is given via a link at the end of the document

Introduction

Although cisplatin and its derivatives are still widely used in the clinic, their side effects, general low solubility and intrinsic or acquired resistance in some cancer types have encouraged research for the discovery of new metal compounds with improved properties.[1,2] From the plethora of transition metal-based compounds synthesized and studied as potential antitumor agents during the last decade, ruthenium derivatives have emerged as promising candidates.[2,3,4–8] Some Ru(III) compounds, NAMI-A (imidazolium trans-[tetrachloridobis(dimethylsulfoxide)(1H-imidazole)-ruthenate(III)),[9] KP1019 (indazolium trans-[tetrachloridobis(1H-indazole)-ruthenate(III)]),[10] and KP1339 (sodium trans-[tetrachloridobis(1H-indazole)-ruthenate(III)])[11] are currently in phase II clinical trials. Organometallic ruthenium(II) arene Supporting information for this article is given via a link at the end of the document complexes such as [(η^6-C_6H_5Ph)Ru(en)Cl][PF_6] (RM175, en = ethylenediamine)[12] and [(η^6-arene)Ru(pta)Cl_2] (pta = 1,3,5-triaza-7-phosphatricyclo[3.3.1]decane; arene = toluene RAPTA-T; arene = *p*-cymene RAPTA-C)[13,14] are also showing great therapeutic promise. In particular, RAPTA-T and RAPTA-C have been shown to have some similar effects to NAMI-A, namely low cell cytotoxicity in vitro, selective anti-tumor activity towards solid metastasizing tumors *in vivo* and remarkable anti-angiogenic properties.[9,14–16] The differences in the anti-carcinogenic properties of structurally similar compounds such as NAMI-A and KP1019, KP1339 or RM175 and RAPTA derivatives show that the ligands bound to the metal assume an important relevance for the activity of the metal based-drugs.[17,18] NAMI-A and RAPTA-T, RAPTA-C compounds seem to act via molecular targets other than DNA,[2,4,19] with different mechanisms of action from those of classical platinum anticancer drugs. In recent years, it has been argued that even for cisplatin, DNA binding is not the only mechanism towards cisplatin-induced apoptosis. The research of possible interactions of metal-based anticancer agents with protein targets that are selective for tumor malignancy are considered a more effective approach to new antitumor drug design.[17,20]

Non-covalent interactions play key roles in biological molecular recognition. Hydrogen bonding, hydrophobic and electrostatic interactions can effectively enhance site-and base-recognition, not only of nucleic acids but also of proteins and enzymes crucial to both metastatic and angiogenic processes.[21,22,23] In this context, oxime groups offer significant advantages for biological applications. They possess stronger hydrogen-bonding capabilities than alcohols or carboxylic acids and have received considerable attention with respect to directional non-covalent intermolecular interactions.[24,25] The presence of hydrogen bonding can also favor solubility of the resulting metal compounds in biological media. In addition, some oxime organic derivatives have been reported to have anticarcinogenic activities, with biological effects such as endothelium-independent relaxation in blood-vessels, an increase in the targeting of specific nuclear bases of DNA and oxidative DNA cleavage.[26] Although oxime and oximate metal derivatives have been extensively studied,[24] their antitumoral properties have received little attention. Oxime-containing Pt(II) compounds have been recently reported as a novel class of nonclassic platinum-based complexes with interesting antitumor properties, different DNA binding behavior and a different pattern of protein interaction from those found in classical cisplatin.[27,28] A variety

of Rh(III) and Ir(III) compounds with oximate ligands have also been studied.[29] The results show a strong cytotoxic effect toward HeLa and HL60 cancer lines, whereas the compounds do not modify DNA in a similar way to that of cisplatin. DNA-binding studies of oxime-containing ruthenium compounds have been previously investigated, but only a weak, non-intercalative in nature interaction was found.[30] However, to the best of our knowledge, the anti-carcinogenic properties of ruthenium oxime compounds have not been reported before.[31]

Examples of enantiopure arene ruthenium anticancer derivatives are scarce in the literature,[32,33,34] probably due to the difficult isolation of unique stereoisomers or enantiomers of organometallic compounds.[34–38] Within this context, enantiomerically pure, naturally occurring terpenes are useful building blocks for asymmetric synthesis.[39,40] They are inexpensive starting reagents, commercially available in optically pure form and easily tailored by stereoselective functionalization.[41] Some of us recently published the stereoselective synthesis of ruthenium compounds with amino-oxime ligands derived from R-limonene.[42] In this work we report a detailed synthetic and NMR study of those and analogous ruthenium compounds, together with a preliminary biological study of the anticarcinogenic properties they have shown against the androgen-unresponsive PC3 cell line.

Results and Discussion

Synthesis and characterization

The reactions of dimer $[(\eta^6\text{-}p\text{-cymene})RuCl_2]_2$ with enantiomerically pure amino-oxime derivatives (2*S*,5*R*)-[NHR,NOH] (R = Ph **a**, Bn **b**)[41,43] afford previously described ruthenium compounds $[(\eta^6\text{-}p\text{-cymene})Ru(k\text{NHR},k\text{NOH})Cl]Cl$,[42] **1a** or **1b**, respectively (Scheme 1). Since compounds **1a** and **1b** are chiral-at-metal derivatives with a new stereogenic center at the amino ligand, four different diastereomers distinguishable by NMR spectroscopy could be formed, namely $R_{Ru}S_N$-(2*S*,5*R*)-[NHR,NOH], $R_{Ru}R_N$-(2*S*,5*R*)-[NHR,NOH], $S_{Ru}S_N$-(2*S*,5*R*)-[NHR,NOH] or $S_{Ru}R_N$-(2*S*,5*R*)-[NHR,NOH]. ^1H and ^{13}C NMR spectra of **1a** and **1b** showed the existence of only one diastereomer in solution, namely $S_{Ru}R_N$-(2*S*,5*R*)-[NHR,NOH]. Reaction of dimer $[(\eta^6\text{-}p\text{-cymene})RuCl_2]_2$ with **a** or **b** was monitored by NMR spectroscopy in chloroform-d_1. ^1H NMR spectra showed the complete conversion of the reactants to only one diastereomer compound after only 5 minutes at room temperature. Epimerization[32,35,36] was never observed in $CDCl_3$, acetone-d_6, methanol-d_4 or D_2O (see supporting information), suggesting a preferred mode of the ligand chelation.[37,44] Stereoselective coordination of potential chelating ligands derived from natural terpenes has been observed before.[40,45]

Following a similar procedure, dimer $[(\eta^6\text{-}p\text{-cymene})RuCl_2]_2$ was reacted with two equivalents of (2*S*,5*R*)-[NH(2-*pic*),NOH] (**c**). The ^1H NMR spectrum in acetone-d_6 or tetrahydrofurane-d_8(THF-d_8) of the resulting solid residue showed a complicated set of resonances which could not be assigned to a unique organometallic derivative. The downfield =NOH proton region showed four broad signals of relative intensities 1:1:1.7:0.8, which could be tentatively assigned to the =NOH proton resonances of four different diastereomers. Having in mind the possible formation of four different diastereomers, as

well as the potential κ^2N,N,N/κ^3N,N,N coordination of the 2-picolylamino-oxime ligand that could produce mono and/or dicationic ruthenium compounds,[8,46] we carried out the reaction in the presence of $TlPF_6$ (Scheme 2). The reaction proceeds in two hours at room temperature to afford a brown suspension, from which a brown solid residue can be extracted with THF or acetone. ^{1}H, ^{13}C and ^{15}N NMR spectra of the solid in acetone-d_6 or THF-d_8 indicate the existence of two different diastereomers of the dicationic complex [(η^6-*p*-cymene)Ru{κ^2NH(2-*pic*),κNOH}][PF_6]$_2$ (**1c**), in a molar ratio of *ca.* 2:1. The lack of stereoselectivity of the synthesis reaction of **1c** compared to **1a, 1b** analogues is probably due to the potential trihapto coordination of the 2-picolylamino-oxime ligand. Such a coordination mode implies displacement of both chloride ligands from the metal center, which could favor formation of configurationally labile solvate derivatives after dissociation of the chlorido ligands and thus, epimerization of the ruthenium compounds.[35]

Both isomers are insoluble in chloroform, dichloromethane or toluene which agrees well with their dicationic character. The relative intensities of each diastereomer do not change in THF-d_8 or acetone-d_6 solution at room temperature or after heating up to 70 °C for several days. While ^{1}H NMR spectrum of the mixture shows a complicated set of overlapped proton signals, ^{13}C NMR displays two well defined set of resonances. Bidimensional ^{15}N-^{1}H HMBC, ^{13}C-^{1}H HSQC and HMBC NMR experiments allowed a full assignment of the proton, carbon and nitrogen resonances displayed (see Supporting Information).

Coordination of the organic derivative **c** to the ruthenium(II) center shifts the ^{13}C NMR signals due to Cq=NOH, CqNH and −CH2-NH groups (δ 179.4, 73.6 and 61.2 (**1c-major**); 175.4, 71.6 and 59.4 (**1c-minor**)) to lower fields in comparison to those signals assigned to the same fragments in the amino-oxime ligand precursor (δ 162.4, 56.9 and 48.1 (**c**)). Upfield shift of the nitrogen resonances arising from the oxime, picoline and amine fragments found in **1c-major** (δ 258.8, 232.7 and 29.9) and **1c-minor** (265.2, 236.4 and 28.9) relative to those observed in **c** (δ 343.3, 305.3 and 51.8) supports the proposed structure for the dicationic ruthenium compounds, with a trihapto-coordination of the picolylamino-oxime derivative to the ruthenium center. A similar upfield shift of the nitrogen signals relative to those observed in the NMR spectra of the ligand precursors was observed for the previously described[42] compounds **1a** and **1b** (see Supporting Information). ^{19}F and ^{31}P NMR spectra of the mixture of **1c-major** and **1c-minor** showed a septuplet and a doublet at δ −144.2 and −72.2 ($J_{P\text{-}F}$ = 708 Hz), respectively, due to PF_6 counter-anions of both isomers, while CHN elemental analysis of the sample agreed well with the proposed composition. The IR spectrum of compound **1c** exhibits strong, broad ν(N-H/O-H) bands at 3642-3500, 3290-3100 cm^{-1} and C=N stretching frequency at 1649, 1614 cm^{-1}, with similar wavenumbers to those bands observed in the IR spectrum of organic derivative **c** (see Supporting Information).

During our experiments, we noticed a strong dependence of the proton NMR chemical shifts of compounds **1a, 1b** and, in a much less degree, **1c**, on the solution concentration. Gradual changes of the chemical shifts of ^{1}H NMR resonances with the variation of concentration have been well documented as a signature of non-covalent interactions leading to self-aggregation behavior in solution.[23,47,48]

Since we were interested in the role of hydrogen bonds on these self-association processes, we synthesized the corresponding amido-oximate compound, which lacks any traditional HB donors, =NOH and −NH. The synthesis of the neutral oximate derivative [(η^6-*p*-cymene)Ru(*k*NHBn,*k*NO)Cl][42] (**2b**) was already reported by a selective deprotonation reaction of equimolar amounts of **1b** and OH (Scheme 3). We performed the reaction of **1b** with NaOMe in a stoichiometric ratio of 1:2, which afforded [(η^6-*p*-cymene)Ru(*k*NBn, k^2NO)] (**3b**), as described in Scheme 3. Treatment of toluene solutions of **2b** with NaOMe in a stoichiometric ratio of 1:1 also afforded pure derivative **3b**. Compound **3b** has been fully characterized by NMR, IR spectroscopy and CHN elemental analysis. The analogous amido derivative [(η^6-*p*-cymene)Ru(*k* NPh, k^2NO)] (**3a**) can be prepared following a similar procedure (see Supporting Information).

Confirmation of the amine deprotonation was provided by IR and ^{15}N-^{1}H HMBC NMR spectroscopic data. IR spectra show the disappearance of the broad absorption in the 3400-3040 cm^{-1} region assigned to ν(NH/NOH), observed in the corresponding spectra of cationic compounds **1a** or **1b** (see supporting information). The C=N stretching frequencies (1622, 1590 cm^{-1}**3a**; 1620, 1601 cm^{-1}**3b**) shift to lower wavenumbers when compared to those found in **1a; 1b** or **2b**, respectively, indicating reduced C=N bond strengths.

Deprotonation of the =NOH oxime function of **1b** to afford derivative **2b**,[42] shifts the ^{15}N NMR resonances from δ 272.0 (**1b**) to 291.7 (**2b**), while keeping the amine nitrogen signal unaltered (δ 50.4 (**1b**), 50.4 (**2b**)) (see Supporting Information). In contrast, ^{15}N-^{1}H HMBC NMR spectra of amido-oximate compounds showed nitrogen resonances at δ 329.0 and 263.5 (**3a**), 328.4 and 256.4 (**3b**) unambiguously assigned to =NO and −RN-Ru nitrogen atoms, respectively.

The strong downfield chemical shift of the nitrogen resonance confirms structural changes on the amine nitrogen atom of **1a** or **1b**, and supports the proposed structure for **3a** or **3b**. The versatility of the oxime groups allows mono *k*N,*k*O, or dihapto k^2NO coordination of nitrogen and oxygen atoms to the metal centers, depending on the nature of the ligands and the metal.[24,27,49] While X-ray structure of compound **2b**[42] and other 18 electron ruthenium oximate derivatives showed a *k*N coordination of the oxime unit,[31,50] a k^2NO coordination is preferred when 16 electron compounds would be formed otherwise[51]

While compounds **1a-C** and **2b** are highly soluble in water[52] (see Supporting Information and Experimental Section) and air-stable for months, **3a** and **3b** remains insoluble in protic solvents and slowly decomposes within a two days period in the presence of air. Derivatives **1a-C** are stable in D_2O for weeks at room temperature. Partial decomposition has only been observed for **1b** after heating the D_2O solutions above 60 °C.

Self-aggregation Behaviour

It is well known that non-covalent interactions play key roles in biological molecular recognition. Thus, we investigated the tendency of these ruthenium compounds to aggregate, considering that they can undergo several non-covalent interactions. H-bond (HB) acceptors (Cl, N and O atoms), HB donors (amino and oxime groups) and carbon atoms with a partial positive charge (aromatic C-H or aliphatic C-H in α position relative to the C=NOH

fragment) are present in **1a-C**. Thus, classical hydrogen bonding and C-H·X interactions can be established. In addition, arene fragments can be involved in π-π stacking interactions.

The concentration dependence of ^{1}H NMR spectral changes was studied for compounds **1a** and **1b**, at 25 °C in $CDCl_3$. Self-association of aromatic frameworks has been studied before by least-squares curve fitting performed on the concentration-dependent ^{1}H NMR resonances, assuming an indefinite self-association or a monomer-dimer model.[48,53]

Least squares curve fitting was performed on the concentration dependent ^{1}H NMR of compounds **1a** and **1b** assuming a dimerization model.[54] Unequivocal ^{1}H NMR assignments of the *p*-cymene resonances were made on the basis of COSY, HSQC and HMBC NMR experiments (see Supporting Information). The selection of the resonances to be studied was a difficult task due to overlapping of some of the aromatic resonances at certain concentrations and broadening of −NH and =NOH corresponding signals. Thus, association constants (K_a) were determined by the least squares curve fitting of the concentration dependent NMR chemical shifts of -CH_2[6] (Figure 1 and 2). Table 1 summarizes the determined association constants. The complicated set of resonances of the ^{1}H NMR spectrum of **1c** precluded the study of the 2-picolylamino-oxime ruthenium compound by this method.

Association constants calculated from aliphatic −CH_2[6] for compound **1b** gave larger K_a than that calculated for compound **1a** (Table 1). Values obtained for ΔG are consistent with the energy of hydrogen bonding.[55]

The self-aggregation tendency of cytotoxic RAPTA and half sandwich diamino Ru(II) salts derivatives has been demonstrated by means of diffusion NMR spectroscopy.[56] In order to further investigate the kind and strength of the non-covalent interactions which are responsible for the self-association processes in our compounds, the translational self-diffusion coefficient (Dt) of the species present in solution was determined by using DOSY NMR measurements. The latter allowed the hydrodynamic radius of the diffusing compounds to be evaluated by taking advantage of the Stockes-Einstein equation.[57] To avoid the measurement of T and η, an internal standard can be used. Thus, only the ratio between self-diffusion coefficients of the sample and the reference is considered, $D_{ref}/D_s = c_s \cdot r_{Hs}/c_{ref} \cdot r_{H(ref)}$.[47,58] The numerical factor c differs significantly with the solvent and the size and shape of the molecule. According to the Zuccaccia results,[56.57] the hydrodynamic radius and the numerical factor c of the reference compound tetrakis(trimethylsilyl)silane (TMSS) can be considered constant in a given solvent within the range of the concentrations studied. Thus, any changes in the translational diffusion coefficients ratio, D_{TMSS}/D_s, can be attributed to modifications in the product $c_s r_{Hs}$ of the sample considered, in a given solvent. In order to check the quality of the results, we used two spherical internal standards, namely TMSS and tetrakis(trimethylsilyloxy)silane (TMSO), which are assumed not to aggregate in solution, thus, the ratios between both, D_{TMSO}/D_{TMSS} should be constant in solutions of different concentration.[58] Saturated solutions of the ruthenium compounds set the upper limit of concentration ranges used, for each given solvent. Table 2 summarizes the data obtained from the DOSY NMR experiments.

Table 2 shows that the calculated relative standard deviation of D_{TMSS}/D_s values is always less than 3% for each given solvent. Since the numerical factor c differs slightly in different solvents,[57] D_{TMSS}/D_s values are expected to vary in some extension when solutions of different solvents are considered. The different D_{TMSS}/D_s values of **1a** and **1b** in $CDCl_3$ or $CDCl_3$:C_6D_6 (8:2) at different concentrations (Table 2, entries 1–4, 11–13) support the conclusion that the compounds self-aggregate in solution.

Although the absolute level of aggregation cannot be inferred without a complete calculation of r_s, Δr_s (see Experimental Part) provide a simplified method for obtaining an indication of the changes on the hydrodynamic radius of the sample considered with the increasing concentrations, and thus, a confirmation of their self-association behavior in solution.

The data indicate smaller variations of Δr_s for **1a** than **1b** (Table 2, entries 1, 2, 11, 13) which is in accordance with the K_a values calculated before.

The effect of solvent was investigated for complex **1a**. Aromatic solvents are known to significantly reduce π-stacking interactions because the solvent molecules effectively solvate the solute.[59] In a similar way, protic solvents decrease hydrogen bond interactions between solute molecules. On the other hand, HB or ion pairs interactions are expected to increase with solvents of low permittivity.[57] Using of $CDCl_3$:C_6D_6 solutions increases variation of Δr_s values at different concentrations of **1a** relative to that found in pure $CDCl_3$ (entries 1–4 in Table 2). This is in line with π-stacking interactions not being the main factor of the aggregation process, which is supported, in the solid state, by the molecular X-ray structure of compound **1a** published before.[42] Stacking interactions of the aromatic fragments are not observed in the ordered extended structures observed for derivative **1a**.

The tendency of **1a** to self-associate with increasing concentration decreases as permittivity solvent increases (as can be inferred from the entries 1–8, of Table 2) which agrees with the main aggregation motif being ion pairing and/or hydrogen bonds interactions.

Since compound **1c** is only soluble in high permittivity solvents, self-aggregation behavior of **1c** could not be assessed in other solvents but acetone-d_6. Variation of Δr_s values for **1c** were similar to that obtained for derivative **1a**, (Table 2, entries 7–10) indicating low changes on their aggregation behavior in that solvent. Accurate DOSY NMR of **1a-1c** in deuterated water at the concentrations range required could not be obtained. Reference compounds TMSS and TMSO are only slightly soluble in water, and their solutions decompose during the DOSY experiments, precluding accurate measurement of their translational diffusion coefficients. However, methanol-d_4 solutions of **1a** could model the aggregation behavior in water of the compounds under study.

The effect of the counter-ion was investigated for cationic complex **1b**. Substitution of chloride by the less coordinating counter-ion $[PF_6]^-$ decreases the variation of Δr_s with solution concentration (Table 2, entries 11–15) while D_{TMSS}/D_s ratios and thus, absolute values of Δr_s, are higher for **1b-PF$_6$** (see Supporting Information) than **1b** at low concentrations, as it has been already demonstrated for other cationic arene ruthenium derivatives with ion pairing effects.[57]

The effect of HB donors =NOH and −NH on the self-association process was studied with derivatives **1b, 2b** and **3b**. Since neutral ruthenium compounds **2b** and **3b** only differ from cation **1b** in one and two hydrogen atoms, respectively, we have assumed that the hydrodynamic radius of the organometallic fragment should be similar for the three compounds, and calculated Δr_s are referred to the compound which affords the lowest D_{TMSS}/D_s values, namely compound **3b** in a 5.82 mM $CDCl_3$ solution.

Aggregation is less affected by increasing concentrations for compound **2b** than **1b**, but D_{TMSS}/D_s ratios and thus, absolute values of Δr_s, are higher for **2b** than **1b** at low concentrations, as it can be deduced from DOSY data summarized in Table 2 (entries 11, 13, 16, 17). Almost no variation on Δr_s was found for compound **3b** at different concentrations (Table 2, entries 18, 19). That fact agrees well with the hydrogen bond interactions being a key factor of self-association, since derivative **2b**, for which no ion pairing contribution can exist, possess stronger HB acceptors (=NO^-) than **1b**, while **3b** lacks of traditional HB donors. The molecular X-ray structure of compound **2b** published before[42] shows intermolecular contacts between the oxygen of the oximate unit and one of the hydrogen atoms of the C**H_3**-CNH of an adjacent molecule, leading to the formation of dimers in the solid state.

Hydrogen bonding has been found to be an important factor in some ion-pair formation of cationic ruthenium compounds.[57,60] A similar behavior might be taking place in compounds **1a,b**, since NMR data allow us to confirm that both interactions are present in solution.

Lipophilicity

Lipophilicity/hydrophobicity is one of the most important physicochemical properties related to the pharmacokinetic behavior of drug-like molecules.[7,61,62] The partition coefficient between water and *n*-octanol (logP) is one of the most commonly used parameters, affording relevant information about the hydrophobicity of compounds. In order to correlate the hydrogen-bonding ability of the compounds and their hydrophilicity, we decided to determine the *n*-octanol/water partition coefficient of derivatives **1a** and **1b** using the shake-flask method[63] at room temperature. The estimated values ($logP_{o/w}$ = 0.40 ± 0.01 (**1a**) and −0.14 ± 0.05 (**1b**)) indicates that **1b** is more hydrophilic than **1a**. This fact agrees with the water solubility of the ruthenium compounds, which follows the order **1a** < **1b** (ca. 21, 28 mM in water, respectively) and correlates with the stronger association capability of **1b** relative to **1a** demonstrated by concentration dependence ^{1}H NMR chemical shifts and DOSY experiments.

NMR Studies under physiological conditions

To elucidate the solution behavior of the compounds under physiological relevant conditions, time-dependent ^{1}H NMR experiments were conducted with **1a-1c** at pH 7.4 in a phosphate buffer saline solution in D_2O.[64] All three compounds proved to be stable under these conditions. Thus, no apparent changes in the NMR spectra were observed during a measurement time of 24, 48 and 72 hours at room temperature or 36 °C (see Supporting Information).

In vitro cell studies

Prostate cancer (PCa) is the most common non-skin cancer among men in developed countries and the second leading cause of cancer death.[65] Although early PCa is generally treatable, most advanced cases eventually progress to a stage characterized by resistance to drugs such as cisplatin and by androgen independence, which jointly contribute to the lack of treatment response and the high mortality rates among patients with advanced PCa.[66] In this regard, bone metastases, with an incidence of 80–90 % in patients at advanced stages of the disease, are the most common cause of death.[67] The *in vitro* effect of the arene ruthenium complexes **1a-1c** on cytotoxicity, cell adhesion and migration of the androgen-independent prostate cancer PC3 cells was assessed by MTT, adhesion to type-I-collagen and recovery of monolayer wounds assays, respectively.

Cytotoxicity activity—The cytotoxic activity of the highly water soluble **1b, b·HCl** and $[(\eta^6\text{-}p\text{-cymene})RuCl_2]_2$ were evaluated as the IC_{50} values after 72 h of incubation (Table 3).

While starting organometallic and proligand products are poorly cytotoxic (IC_{50} > 170 μM), the water soluble ruthenium amino-oxime compound shows considerable higher cytotoxicity than cisplatin (51 ± 0.10 μM, under the same experimental conditions[68,69]).

Antiproliferative effect of derivative **1b** was also assessed at different exposure times (3 h and 24 h), revealing a high cytotoxic activity against PC3 cells after 3h of incubation (IC_{50} = 14.8 ± 0.40, Table 3). Treatment with ruthenium compounds **1a, 1b** and **1c** for 3 h significantly decreased cell viability in PC3 cells as compared with control conditions, showing an inhibitory activity of 75–82% at concentrations of 50 μM, with calculated IC_{50} values in the low micromolar concentration range (Figure 3, Table 3). In order to compare the effect on cell viability of the starting material $[(\eta^6\text{-}p\text{-cymene})RuCl_2]_2$ and of the ligand precursors, with that of organometallic compounds **1a- 1c**, the ruthenium dimer and water soluble organic ammonium-oximes were also studied under the same experimental conditions (Figure 3 and supporting information). They showed a decrease of only 13–18% on PC3 cell viability at the same concentrations (50 μM) which confirms that coordination of amino-oxime derivatives to ruthenium lead to compounds with significantly enhanced activity.

Some other ruthenium compounds have proved their antitumor activity against PC3 cells line, known for their chemoresistance.[62,69,70] To the best of our knowledge, the most successful ruthenium derivative tested *in vitro* is the cyclopentadienyl cationic derivative $[(\eta^5\text{-}C_5H_5)Ru(bipy)(PPh_3)][CF_3SO_3]$ (TM34,[69] bipy = bipyridine), with IC_{50} values of 0.54 ± 0.10 μM after 72 hours of incubation, almost 100-folds more cytotoxic against PC3 when compared to cisplatin.[68,69] The water-soluble version of the compound, $[(\eta^5\text{-}C_5H_5)Ru(bipy)(mTPPMSNa)][CF_3SO_3]$ (TM85, bipy = bipyridine, mTPPMS = diphenylphosphane-benzene-3-sulfonate) was evaluated in a variety of cell lines. The IC_{50} value found for the PC3 cell line was 25.8 ± 8.5 μM after a 72 h exposure.[62]

Adhesion to collagen—We performed experiments on cell adhesion to type-I collagen in order to determine the effect of **1a, 1b** and **1c** on metastatic capability of androgen-independent prostate cancer cells under conditions which did not cause cell death. To

investigate the cell adhesion *in vitro*, we incubated PC3 cells in the absence or presence of 20 μM of **1a** and **1c** and 10 μM of **1b** on a collagen plate. PC3 cells rapidly adhered to collagen basement in 40 min and showed a significant increase of the cell adhesion to collagen after treatment with **1a** (18 %), **1b** (46 %) and **1c** (45 %) compared to that observed for control cells. The arene ruthenium dimer and ammonium-oxime derivatives-treated cells exhibited an adhesion pattern similar to that of control cells (Figure 4).

Wound-healing assay—The wound-healing assay is a useful method for gauging the anti-migratory activity of drug candidates.[71] In order to evaluate cell migration we performed wound-healing assays, in which a small wound area was made on the plate with a confluent monolayer of cells (Figure 5). After 24 h, the cells treated with the ruthenium complexes **1a, 1b** and **1c** (5 μM) showed a lower migration capability (60% of wound healing) than that of control cells. The ruthenium dimer and ammonium-oxime treated cells showed a migration pattern similar to that of control cells (5 % of wound healing). Our results confirmed the inhibitory effect of compounds **1a-1c** on prostate tumor cell migration. In this regard, the treatment of human umbilical vein endothelial cells with organometallic ruthenium(II) compounds RAPTA-C, DAPTA-C and DAPTA-T for 6 h reveals a similar migratory capability using a concentration ten times higher than that used in our study.[16]

The amino-oxime Ru(II) complexes seem to modulate both adhesion and migratory capabilities of PC3 cells affecting metastatic phenotype. It is worth noting that compound **1b**, which has demonstrated higher self-aggregation than **1a** in solution, showed also the best anti-cancer activity.

Reactivity with biomolecules

Interactions with plasmid DNA—Since DNA replication is a key event for cell division, it is among critically important targets in cancer chemotherapy. Most cytotoxic platinum drugs form strong covalent bonds with the DNA bases.[72] However, a variety of platinum compounds act as DNA intercalators upon coordination to the appropriate ancillary ligands.[73] The more thoroughly studied ruthenium antitumor agents have displayed differences with respect to their interactions with DNA depending on their structure.[5] Thus, while NAMI-A is known to have fewer and weaker interactions with DNA than cisplatin,[5] KP1019 undergoes interactions similar to cisplatin but with a lower intensity in terms of DNA-DNA and DNA-protein crosslinks.[74] Organometallic piano-stool ruthenium(II) compounds based on bicyclic arenes RM175 interact strongly with DNA binding to guanines and by intercalation.[21,75] Organometallic ruthenium(II) RAPTA derivatives, characterized by the presence of water soluble PTA phosphine, exhibit pH-dependent DNA damage: at the pH typical of hypoxic tumor cells DNA was damaged, whereas at the pH characteristic of healthy cells little or no damage was detected.[76] It is also known that some metal compounds containing oxime ligands cause oxidative DNA cleavage,[77] and an increase in the targeting of specific nuclear bases of DNA[78]

In this context, we performed agarose gel electrophoresis studies to unravel the effects of the water soluble ammonium-oxime ligands **a·HCl-c·HCl** and ruthenium complexes **1a-1c** on

plasmid (pBR322) DNA (Figure 6). Cisplatin and the starting dimeric organometallic ruthenium complex $[(\eta^6\text{-}p\text{-cymene})RuCl_2]_2$ were also measured as controls.

Plasmid (pBR322) DNA has two main forms: OC (open circular or relaxed form, Form II) and CCC (covalently closed or supercoiled form, Form I). Changes in electrophoretic mobility of both forms are usually taken as evidence of metal-DNA binding. Generally, the larger the retardation of supercoiled DNA (CCC, Form I), the greater the DNA unwinding produced by the drug.[79] Binding of cisplatin to plasmid DNA, for instance, results in a decrease in mobility of the CCC form and an increase in mobility of the OC form (see lanes 1–4 for cisplatin in Figure 6).

Treatment with increasing amounts of derivatives **a·HCl-c·HCl** and ruthenium compounds **1a-1c** do not affect the mobility of the faster-running supercoiled form (Form I) even at the highest molar ratios (lane 4, Figure 6). In conclusion, the experiments probing DNA-drug interactions showed that the biologically active ruthenium complexes have no or very little interaction with plasmid (pBR322) DNA, pointing to an alternative biomolecular target for these compounds.

This is also in accordance with previous reports on other coordination Ru(II) complexes[30] and organometallic Rh(III) and Os(III)[29] derivatives containing oxime groups which showed no or weak interaction with DNA by different techniques.

In addition, to evaluate the possible interaction of the new ruthenium complexes **1a-1c** with DNA some Thermal Denaturation experiments were carried out. The melting technique is a sensitive and easy tool to detect even slight DNA conformational changes. It is known that a destabilizing interaction with the double helix (typically, covalent) produces a decrease in the Tm, while a stabilizing interaction (usually by intercalation or by electrostatic attraction) induces an increase of the Tm. Bearing that in mind, Calf Thymus DNA was incubated for 1 hour with each drug at a DNA:drug ratio of 2:1. The results are summarized in Table 4.

Complex **1a** was not able to modify the melting temperature of a solution of calf thymus DNA beyond the experimental error while the modification of the temperature with **1c** (1 °C) indicates a very weak interaction with double-stranded DNA, most likely of electrostatic nature.[80] This fact suggests that these compounds do not interact with DNA or that interaction is so weak that cannot be detected by this technique, supporting the results obtained in the study of the interaction of these compounds with plasmid (pBR322) DNA. In summary, it seems that the cytotoxic effects of the ruthenium compounds **1a-1c** are not solely related to DNA damage which suggests that an alternative cellular death pathway may be taking place.

Interactions with HSA—Human serum albumin (HSA) is the most abundant carrier protein in plasma and is able to bind a variety of substrates including metal cations, hormones and most therapeutic drugs. It has been demonstrated that the distribution, the free concentration and the metabolism of various drugs can be significantly altered as a result of their binding to the protein.[74]

HSA possesses three fluorophores, these being tryptophan (Trp), tyrosine (Tyr) and phenylalanine (Phe) residues, with Trp214 being the major contributor to the intrinsic fluorescence of HSA. This Trp fluorescence is sensitive to the environment and binding of substrates, as well as changes in conformation that can result in quenching (either dynamic or static). Thus, the fluorescence spectra of HSA in the presence of increasing amounts of compound **1a-1c**, the ruthenium starting material [(η^6-*p*-cymene)$RuCl_2$]2 and cisplatin were recorded in the range of 300–450 nm upon excitation of the tryptophan residue at 295 nm. All the compounds caused a concentration dependent quenching of fluorescence without changing the emission maximum or shape of the peaks as seen in Figure 7(A) for compound **1a**.

The quenching was more significant for the dimer [(η^6-*p-cymene*)$RuCl_2$]$_2$ and Ru(II) complexes **1a-1c** than for cisplatin under the chosen conditions. This is most likely due to a faster reactivity of the organometallic ruthenium compounds with HSA compared to cisplatin.

The fluorescence data was analyzed by the Stern-Volmer equation. While a linear Stern-Volmer plot is indicative of a single quenching mechanism, either dynamic or static, the positive deviation observed in the plots of F_0/F versus [Q] of **1a** or **1b** (Figure 7(B)) suggests the presence of different binding sites in the protein.[81] A similar behavior was observed for iminophosphorane complexes of Ru(II),[6] Pd(II) or Pt(II)[82] reported by some of us. In the case of [MCl_2(TPA=N-C(O)-2-NC_5H_4)] (M = Pd, Pt), isothermal titration calorimetry (ITC)[82] showed two different binding interactions which explained the lack of linearity observed in the fluorescence quenching studies, as the Stern-Volmer method assumes all binding sites to be equivalent.

We believe that a similar reactivity takes place for the compounds described here. In contrast, the Stern-Volmer plot for complex **1c** shows a linear relationship, suggesting the existence of a single quenching mechanism and a single binding affinity. The Stern-Volmer constant for **1c** is 1.17×10^6 M^{-1}.

Conclusions

The self-association tendency of the compounds **1a-1c** has been studied by means of concentration dependence and DOSY ^{1}H NMR spectroscopy experiments. Hydrogen bond interactions seem to be a key factor in the observed process in solution. Furthermore, our study has shown that the use of amino-oxime ligands is a useful strategy to design water-soluble metal compounds. The oxime-containing Ru(II) derivatives did not display an interaction with plasmid (pBR322) DNA and their interaction with calf-thymus DNA seems very weak or nonexistent. The compounds **1a** and **1b** interact with HSA faster than cisplatin and most plausibly through more than one binding site. This different behavior along with very promising *in vitro* results on cytotoxicity, cell adhesion and migration of the androgen-independent cisplatin-resistant prostate cancer PC3 cell line makes these compounds attractive candidates for further testing as potential prostate chemotherapeutic agents.

Experimental Section

Synthesis of metal complexes **1a-C** and **2b** were performed without exclusion of moisture or air. Manipulations involving synthesis of metal complexes **3a** and **3b** were performed at an argon/vacuum manifold using standard Schlenk techniques or in a glove-box MBraun MOD System. Solvents were dried by known procedures and used freshly distilled. (2S,5R)-[NHR,NOH], (R = Ph **a**, Bn **b**, 2-*pic* **c**), corresponding adducts (2S,5R)-[NHRHCl,NOH], (R = Ph **a·HCl**, Bn **b·HCl**, 2-*pic* **c·HCl**), [(η^6-*p*-cymene)Ru(*k*NHR,*k*NOH)Cl]Cl (R = Ph **1a**, Bn, **1b**) and [(η^6-*p*-cymene)Ru(*k*NHBn,*k*NO)Cl] **2b** were prepared according to previous reports.[41,42] Tetrakis(trimethylsilyl)silane (TMSS), tetrakis(trimethylsilyloxy)silane (TMSO), sodium methoxide (NaOMe), [(η^6-*p*-cymene)$RuCl_2$]$_2$, cisplatin, KCl, NaCl, Na_2HPO_4, KH_2PO_4 and DCl solution in D_2O were purchased from Sigma-Aldrich. Commercially available reagents were used without further purification. NMR spectra were recorded on a Bruker 400 Ultrashield. ^{1}H and ^{13}C chemical shifts are reported relative to tetramethylsilane. ^{15}N chemical shifts are reported relative to liquid ammonia (25 °C). Coupling constants *J* are given in Hertz. Elemental analyses were performed in our laboratories (UAH) on a Perkin Elmer 2400 CHNS/O Analyzer, Series II. IR spectra were recorded on IR FT Perkin Elmer (Spectrum 2000) spectrophotometer on KBr pellets; only significant bands are cited in the text. pH was measured in a HANNA HI208 pHmeter in distilled water solutions.

NMR experiments

Dilutions experiments were carried out from an initial 500 μL stock solution. This initial stock solution was diluted with $CDCl_3$ (100 μL), and the dilution process sequentially repeated for the next 9 samples. OriginLab Software was used for least-squares curve fitting to the theoretical equation of the dimerization model (Supporting Information). DOSY experiments were acquired in a Bruker Ultra Shield 400 spectrometer, using the ledbpgp2s pulse program. The gradient strength (g) was the variable parameter, while Δ (diffusion time) and δ (diffusion gradient length) were kept constant during the 2D-DOSY study. Appropriate Δ and δ values were selected for each sample by optimization of the attenuation of the ^{1}H NMR signals in 1D-versions of the diffusing ledbpgp1s pulse program. The values of Δ and δ were 40–100 ms and 1.5–2.5 ms, respectively; depending on the sample and the solution concentration (eddy current delay was set to 5 ms in all the experiments). The pulse gradients (g) were incremented from 2 to 95% of the maximum gradient strength in a linear ramp. The diffusion dimension was processed with Bruker topspin T1/T2 software. Δr_s values were calculated according to the equation 1, considering C_i and C_0 the highest and lowest concentration studied for each compound in a given solvent, respectively, and assuming that the product $\mathbf{C}_{TMSS}\cdot\mathbf{r}_{TMSS}$ is not concentration-dependent.

$$\frac{\left[\frac{D_{TMSS}}{D_S}\right]_{C_i}}{\left[\frac{D_{TMSS}}{D_S}\right]_{C_0}} = \frac{\left[c_{TMSS}\cdot r_{TMSS}\right]_{C_0}}{\left[c_{TMSS}\cdot r_{TMSS}\right]_{C_i}} \cdot \frac{\left[c_s\cdot r_s\right]_{C_i}}{\left[c_s\cdot r_s\right]_{C_0}} = \frac{\left[c_s\cdot r_s\right]_{C_i}}{\left[c_s\cdot r_s\right]_{C_0}} = \Delta r_s \quad (1)$$

Synthesis of [(η^6-*p*-cymene)Ru{κ^2NH(2-*pic*),*k*NOH}][PF_6]$_2$ (1c)

A THF (10 mL) solution of (2*S*,5*R*)-{NH(2-*pic*),NOH} (0.27 g, 0.98 mmol) and [(η^6-*p*-cymene)$RuCl_2$]$_2$ (0.30 g, 0.49 mmol) was stirred for 30 minutes at room temperature and then treated with $TlPF_6$ (0.68 g, 1.96 mmol). After stirring of the mixture for two hours, the brown suspension was filtered to afford a brown solution. Evaporation of the solvent affords a brown-deep solid. The solid was purified by column chromatography. Elution with acetone allowed isolation of derivative **1c** (yield 0.25 g, 63 %). NMR data confirmed the presence of two different isomers, **1c-major** and **1c-minor** in a 2:1 ratio. Solubility in H_2O at 24 °C (mM): 9.0 ± 1. Value of pH ([9.0 mM]) in H_2O at 24 °C: 4.00. $C_{26}H_{37}N_3ORuP_2F_{12}$ (798,56): calcd. C 39.10, H 4.67, N 5.26; found: C 38.81, H 4.58, N 5.11. IR (KBr): ν = 3642-3500, 3290-3100 (NH/NOH), 1649, 1614 (C=N) cm^{-1}. ^{19}F NMR (376.5 MHz, 293 K, acetone-d_6): δ = −72.2 (d, J_{P-F} = 708, PF_6) ppm. ^{31}P NMR (161.9 MHz, 293 K, acetone-d_6): δ = −144.2 (spt, J_{P-F} = 708, PF_6) ppm. Since many of the ^1H NMR resonances were overlapped, full assignment was only possible with bidimensional ^1H-^{13}C experiments (see Supporting Information for details). **1c-major:** ^1H NMR (plus HSQC, plus HMBC, 400.1 MHz, 293 K, acetone-d_6): δ = 11.76 (br, overlapped, NOH), 9.45, 8.21, 7.90, 7.75 (all m, overlapped, C_5H_4N), 7.76 (overlapped, NH), 6.49, 6.33, 6.26, 6.19 (all m, overlapped, *p*-cymene-C_6H_4), 5.06, 5.16 (both s, each 1H, =CH_2), 5.16 (d, J_{HH} = 17, 1H, *pic*-CH_2), 4.76 (dd, J_{HH} = 5, J_{HH} = 17, 1H, *pic*-CH_2), 3.61, 2.37, 2.24, 2.15, 2.13, 1.97 (all m, overlapped, -$CH_2^{3,4,6}$), 2.77 (m, 1H, −CH-C=), 2.75 (spt, J_{HH} = 6, overlapped, *p*-cymene-$CHMe_2$), 2.19, 1.85, 1.43 (all s, *p*-cymene-CH_3 + *pic*NC-CH_3 + CH_3C=), 1.16, 1.09 (both d, J_{HH} = 6, overlapped, *p*-cymene-CH(CH_3)$_2$) ppm. ^{13}C- NMR (plus APT, plus gHSQC, plus HMBC, 100.6 MHz, 293 K, acetone-d_6): δ = 179.4 (−, Cq=N), 162.0 (−, Cipso-C_5H_4N), 156.8, 142.9, 128.1, 124.5 (+, −NC_5H_4), 147.2 (−, =Cq-Me), 113.6 (−, =CH_2), 110.4, 105.5 (both −, C_{ipso}-*p*-cymene), 89.0, 88.2, 87.6, 86.6 (+, −C_6H_4), 73.6 (−, Cq-NH), 61.2 (−, *pic*-CH_2), 43.2 (+, −CH^5), 38.9, 25.3, 29.6 (all −, − $CH_2^{3,4,6}$), 32.2 (+, *p*-cymene-$CHMe_2$), 23.2, 21.9, 19.4 (all +, CH_3-CNH + CH_3-C= + CH_3-C_6H_4), 23.4, 22.9 (+, *p*-cymene-CH(CH_3)$_2$) ppm. ^{15}N NMR (gHMBC, 40.5 MHz, 293 K, acetone-d_6): δ = 258.8 (C=N), 232.7 (NC_5H_4), 29.9 (NH) ppm. **1c-minor**: ^1H NMR (plus HSQC, plus HMBC, 400.1 MHz, 293 K, acetone-d_6): δ = 11.76 (br, NOH), 9.45, 8.21, 7.90, 7.75 (all m, overlapped, C_5H_4N), 7.76 (overlapped, NH), 6.53, 6.41, 6.41, 6.33 (all m, overlapped, *p*-cymene-C_6H_4), 3.98, 3.32 (both s, each 1 H, =CH_2), 5.02 (d, J_{HH} = 17, 1H, *pic*-CH_2), 4.59 (dd, J_{HH} = 5, J_{HH} = 17, 1H, *pic*-CH_2), 3.37, 2.57, 2.15, 1.97, 1.97, 1.87 (all m, overlapped, −$CH_2^{3,4,6}$), 2.82 (spt, J_{HH} = 7, overlapped, *p*-cymene-$CHMe_2$), 2.51 (m, 1H, −CH-C=), 2.26, 1.77, 1.48 (all s, each 3H, *p*-cymene-CH_3 + *pic*NC-CH_3 + CH_3C=), 1.23, 1.16 (both d, J_{HH} = 7, overlapped, *p*-cymene-CH(CH_3)$_2$) ppm. ^{13}C- NMR (plus APT, plus gHSQC, plus HMBC, 100.6 MHz, 293 K, acetone-d_6): δ = 175.4 (−, Cq=N), 161.1 (−, Cipso-C_5H_4N), 156.4, 142.9, 127.9, 125.3 (+, −NC_5H_4), 146.0 (−, =Cq-Me), 111.2 (−, =CH_2), 110.7, 104.6 (both −, C_{ipso}-*p*-cymene), 89.1, 88.7, 87.9, 86.7 (+, −C_6H_4), 71.6 (−, Cq-NH), 59.4 (−, *pic*-CH_2), 40.3 (+, −CH^5), 32.1, 29.5, 26.8 (all −, −$CH_2^{3,4,6}$), 32.9 (+, *p*-cymene-$CHMe_2$), 27.5, 21.7, 19.1 (all +, CH_3-CNH + CH_3-C= + CH_3-C_6H_4), 24.5, 22.3 (+, *p*-cymene-CH(CH_3)$_2$) ppm. ^{15}N NMR (gHMBC, 40.5 MHz, 293 K, acetone-d_6): δ = 265.2 (C=N), 236.4 (NC_5H_4), 28.9 (NH) ppm.

Synthesis of [(η^6-*p*-cymene)Ru(*k*NBn,*k*^{2}NO)] (3b)

A THF solution of **1b** (0.27 g, 0.47 mmol) was treated with NaOMe (0.05 g, 0.98 mmol) at room temperature. After stirring of the mixture during 2 hours, evaporation of the THF and extraction from the solid residue with toluene affords an orange solution from which an orange solid was isolated, washed with hexane (5×2 mL) and fully characterized as derivative **3b** (yield 0.22 g, 92 %). Alternatively, a toluene solution of **2b** (0.20 g, 0.37 mmol) was treated with NaOMe (0.02 g, 0.37 mmol) at room temperature. After stirring of the mixture during 2 hours, the resulting suspension was filtered and the solvent evaporated to dryness to afford an orange solid which was identified as derivative **3b**. $C_{27}H_{36}N_2ORu$ (505.66): calcd. C 64.13, H 7.18, N 5.54; found C 63.81, H 6.87, N 5.09. IR (KBr): ν = 1620, 1600 (νC=N) cm^{-1}. ^{1}H NMR (plus COSY, plus HSQC, 400.1 MHz, 293 K, $CDCl_3$): δ = 7.37 (overlapped, 5H, $-C_6H_5$), 5.20 (d, 1H, $^3J_{HH}$ = 6, *p*-cymene-C_6H_4), 5.09 (br, 1H, $=CH_2$), 4.95, 4.84 (both d, each 1H, $^3J_{HH}$ = 6, *p*-cymene-C_6H_4), 4.72 (br, 1H, $=CH_2$), 4.66 (d, 1H, $^3J_{HH}$ = 6, *p*-cymene-C_6H_4), 4.47 (m, 2H, $-CH_2$Ph), 3.87 (d, 1H, $^2J_{HH}$ = 14, $-CH_2^6$), 2.57 (spt, 1H, $^3J_{HH}$ = 6, *p*-cymene-$CHMe_2$), 2.40 (br, 1H, $-CH^5$), 2.08 (s, 3H, *p*-cymene-CH_3), 1.85 (dd, 1H, $^2J_{HH}$ = 16, $^3J_{HH}$= 6, $-CH_2^6$), 1.79 (m, 1H, $-CH_2^3$), 1.64 (m, 1H, $-CH_2^4$), 1.60 (s, 3H, CH_3-C=), 1.55 (m, 1H, $-CH_2^4$), 1.24, 1.22 (both d, each 3H, $^3J_{HH}$ = 6, *p*-cymene-$CH(CH_3)_2$), 1.10 (overlapped, 4H, NC-CH_3 + $-CH_2^3$) ppm. ^{13}C-NMR (plus APT, plus gHSQC, 100.6 MHz, 293 K, $CDCl_3$): δ = 163.4 (−, C=NO), 144.9, 144.2 (both −, C=CH_2 + C_{ipso}-Bn), 128.6, 128.5, 127.0 (all +, $-C_6H_5^{o,m,p}$), 112.2 (−, $=CH_2$), 98.9, 88.8 (both −, C_{ipso}-*p*-cymene), 84.6, 84.0, 83.5, 80.7 (+, *p*-cymene-C_6H_4), 80.4 (−, C-NBn), 64.0 (−, CH_2Ph), 42.1 (+, $-CH^5$), 32.7 (−, $-CH_2^3$), 31.8 (+, *p*-cymene-$CHMe_2$), 26.5 (−, $-CH_2^4$), 25.3 ($-CH_2^6$), 24.1, 24.1 (both +, *p*-cymene-$CH(CH_3)_2$), 23.4 (+, $-CH_3$-CNBn), 22.8 (+, CH_3-C=), 19.8 (+, *p*-cymene-CH_3) ppm. ^{15}N NMR (gHMBC, 40.5 MHz, 293 K, $CDCl_3$): δ = 328.4 (C=NO), 256.4 (Ru-NBn) ppm.

Biological assays

***n*-octanol-water partition coefficients—**The n-octanol-water partition coefficient was measured using the shake-flask method.[63] Distilled water and *n*-octanol were stirred together for 72 h at 25 °C, to promote saturation of both phases. The solvents were separated and freshly used. Aliquots of stock solutions (1.5mM) of **1a** and **1b** in the *n*-octanol saturated aqueous phase were added to equal volumes of water saturated *n*-octanol and shaken on a mechanical shaker for 1 h. The resultant biphasic solution was centrifuged to separate the layers, and UV-vis absorption spectra of both solutions were registered in both phases in a Cary 100 Bio UV-visible spectrophotometer at 411 nm and compared with a calibration curve to obtain the compound concentration of **1a** and **1b** in both phases. LogP was defined as the logarithm of the ratio $[Ru]_{ocanol}/[Ru]_{water}$; values reported are the means of three separate experiments.

Cell line and culture conditions—The androgen-unresponsive cell line PC3 was obtained from the American Type Culture Collection (Manassas, VA) and may be related to recurrent prostate cancers that have achieved androgen independence. All culture media were supplemented with 1% penicillin/streptomycin/amphoterycin B (Life Technologies, Barcelona, Spain). The culture was performed in a humidified 5% CO_2 environment at 37 °C. After the cells reached 70–80% confluence, they were washed with phosphate

buffered saline (PBS), detached with 0.25% trypsin/0.2% EDTA and seeded at 30,000–40,000 cells/cm^2. The culture medium was changed every 3 days.

Cytotoxicity assays—PC-3 (4×10^4) cells were grown in 24-well plates. After 24 h, the culture medium was removed and replaced with RPMI-1640 medium containing 10% fetal bovine serum (FBS) and 1% penicillin/streptomycin/amphotericin B for 24 h. Stock solutions of compounds **1a-1c** (up to 300 μM) were prepared in complete medium and used for sequential dilutions to desired concentrations. Stock solutions of compounds **a·HCl-c·HCl** and $[(\eta^6\text{-p-cymene})RuCl_2]_2$ were freshly prepared in DMSO (100 μL), diluted in complete medium (50 mL) up to 800 and 1000 μM, respectively, and used for sequential dilutions to desired concentrations. The final concentration of DMSO in the cell culture medium did never exceed 0.5%. Control groups with and without DMSO (0.5%) were included in the assays.

The cytotoxic activity of the chemical compounds was screened against PC3 cell line within a wide concentration range depending on the exposure time, using MTT [3-(4,5-dimethylthiazol-2-yl)-2,5-diphenyltetrazolium bromide] colorimetric assay. Cell growth was determined by a tetrazolium assay, which measures the reduction of substrate MTT [3-(4,5-dimethylthiazol-2-yl)-2,5-diphenyltetrazolium bromide] to a dark blue formazan product by mitochondrial dehydrogenases in living cells. Isopropanol was added to each well to dissolve the formazan precipitates and absorbances were read at 570 nm using the plate reader ELX 800 (Bio-Tek Instruments, Winooski, VT) with a reference wavelength at 620 nm. Each experiment was repeated at least three times and each concentration was tested in at least six replicates. Results are expressed as a percentage of survival with respect to control cells in the absence of the compound. IC_{50} values (half-inhibitory concentration) were calculated from curves constructed by plotting cell survival (%) *versus* compound concentration (M). The IC_{50} values were calculated with the GraphPad Prism software.

Cell adhesion assay—Concentrated type-I collagen solution was diluted in 10 mM glacial acetic acid and coated onto 96-well plates for 1 h at 37°C Plates were washed twice with PBS (pH 7.4). Cells were harvested with 0.25% trypsin/0.2% EDTA and collected by centrifugation. They were suspended in RPMI medium/0.1% (w/v) bovine serum albumin (BSA) (pH 7.4) and treated with the complexes for 30 min. Then, cells plated at 2.5×10^4 cells per 100 μl. The assay was terminated at indicated time intervals by aspiration of the wells. Cell adhesion was quantified by MTT colorimetric assay as mentioned above.

Wound-healing assay—PC3 cells were incubated in 24-well plates and a small wound area was made with a scraper in the confluent monolayer. Afterwards, cells were incubated in the absence or presence of the complexes. Four representative fields of each wound were captured using a Nikon Diaphot 300 inverted microscopy at different times (0–24 h). Wound areas of untreated samples were averaged and assigned a value of 100%.

Data analysis—Data were subjected to one-way ANOVA and differences were determined by Bonferroni's multiple comparison test. Each experiment was repeated at least three times. Data are shown as the means of individual experiments and presented as the mean 6 S.E.M.; $P < 0.05$ was considered statistically significant.

Interactions with biomolecules—Calf Thymus DNA, plasmid (pBR322) DNA, HSA and buffers were purchased from Sigma-Aldrich. Electrophoresis experiments were carried out in a Bio-Rad Mini sub-cell GT horizontal electrophoresis system connected to a Bio-Rad Power Pac 300 power supply. Photographs of the gels were taken with an Alpha Innotech FluorChem 8900 camera. Thermal denaturation experiments were performed on an Agilent 8453 diode-array spectrophotometer equipped with a HP 89090 Peltier temperature control accessory. Fluorescence intensity measurements were carried out on a PTI QM-4/206 SE Spectrofluorometer (PTI, Birmingham, NJ) with right angle detection of fluorescence using a 1 cm path length quartz cuvette.

Mobility Shift Assay—10 μL aliquots of pBR322 plasmid DNA (20 μg/mL) in buffer (5 mM Tris/HCl, 50 mM $NaClO_4$, pH = 7.39) were incubated with different concentrations of the compounds (**a·HCl-c·HCl, 1a-1c** and $[(\eta^6\text{-p-cymene})RuCl_2]_2$) (in the range 0.25 and 4.0 metal complex:DNAbp) at 37 °C for 20 h in the dark. Samples of free DNA and cisplatin-DNA were prepared as controls. After the incubation period, the samples were loaded onto the 1 % agarose gel. The samples were separated by electrophoresis for 1.5 h at 80 V in Tris-acetate/EDTA buffer (TAE). Afterwards, the gel was stained for 30 min with a solution of GelRed Nucleic Acid stain.

Thermal Denaturation Experiments—Melting curves were recorded in media containing 50 mM $NaClO_4$ and 5 mM Tris/HCl buffer (pH = 7.39). The absorbance at 260 nm was monitored for solutions of Calf Thymus DNA (35 μM) before and after incubation with a solution of the drug under study (17.5 μM in Tris/HCl buffer) for 1 h at room temperature. The temperature was increased by 0.5 °C/min between 65 and 82 °C and by 3 °C/min between 25 and 65 °C and between 82 and 97 °C.

Fluorescence Spectroscopy—An solution of each compound (8 mM) was prepared and ten aliquots of 2.5 μL were added successively to a solution of HSA (10 μM) in phosphate buffer (pH = 7.4) to achieve final metal complex concentrations in the range 10–100 μM. The excitation wavelength was set to 295 nm, and the emission spectra of HSA samples were recorded at room temperature in the range of 300 to 450 nm. The fluorescence intensities of the metal compounds and the buffer are negligible under these conditions. The fluorescence was measured 240 s after each addition of compound solution. The data were analyzed using the classical Stern-Volmer equation $F_0/F = 1 + K_{SV}[Q]$.

Supplementary Material

Refer to Web version on PubMed Central for supplementary material.

Acknowledgments

Financial support from the Ministerio de Economía y Competitividad of Spain (MINECO, I3 Program, Project 3090XF067) and the Universidad de Alcalá (UAH, Project CCG2013/EXP-056) is acknowledged. Y.B. acknowledges Agencia Española de Cooperación Internacional (AECI) for fellowship. Brooklyn College (The City University of New York) authors thank the National Cancer Institute (NCI) for grant 1SC1CA182844 (M.C.). E.R. would like to thank Dr. M. del Camino González-Arellano (UAH) for fruitful discussions on the aggregation studies in solution.

References

1. Keppler, BK. Metal Complexes in Cancer Chemotherapy. Weinheim: Wiley VCH; 1993. Barnes, KR.; Lippard, SJ. Metal Ions in Biological Systems. Sigel, A.; Sigel, H., editors. Vol. 42. Marcel Dekker Inc; 2004. p. 179-208.van Rijt SH, Sadler PJ. Drug Discov. Today. 2009; 14:1089–1097. [PubMed: 19782150] Gasser G, Ott I, Metzler-Nolte N. J. Med. Chem. 2011; 54:3–25. [PubMed: 21077686] Hartinger CG, Metzler-Nolte N, Dyson PJ. Organometallics. 2012; 31:5677–5685.
2. Sava G, Bergamo A, Dyson PJ. Dalton Trans. 2011; 40:9069–9075. [PubMed: 21725573]
3. Melchart, M.; Sadler, PJ. Bioorganometallics. Jaouen, G., editor. Weinheim: Wiley VCH Verlag GmbH & Co. KGaA; 2006. p. 39-64.Bergamo A, Sava G. Dalton Trans. 2011; 40:7817–7823. [PubMed: 21629963] Smith GS, Therrien B. Dalton Trans. 2011; 40:10793–10800. [PubMed: 21858344] Clavel CM, Paunescu E, Nowak-Sliwinska P, Griffioen AW, Scopelliti R, Dyson PJ. J. Med. Chem. 2014; 57:3546–3558. [PubMed: 24669938] Nazarov AA, Hartinger CG, Dyson PJ. Journal of Organometallic Chemistry. 2014; 751:251–260.Pettinari R, Marchetti F, Condello F, Pettinari C, Lupidi G, Scopelliti R, Mukhopadhyay S, Riedel T, Dyson PJ. Organometallics. 2014; 33:3709–3715.
4. Ang WH, Casini A, Sava G, Dyson PJ. J. Organomet. Chem. 2011; 696:989–998.
5. Bergamo A, Gaiddon C, Schellens JHM, Beijnen JH, Sava G. J. Inorg. Biochem. 2012; 106:90–99. [PubMed: 22112845]
6. Frik M, Martinez A, Elie BT, Gonzalo O, de Mingo DR, Sanau M, Sanchez-Delgado R, Sadhukha T, Prabha S, Ramos JW, Marzo I, Contel M. J. Med. Chem. 2014; 57:9995–10012. [PubMed: 25409416]
7. Aman F, Hanif M, Siddiqui WA, Ashraf A, Filak LK, Reynisson J, Sohnel T, Jamieson SMF, Hartinger CG. Organometallics. 2014; 33:5546–5553.
8. Sommer MG, Kureljak P, Urankar D, Schweinfurth D, Stojanovic N, Bubrin M, Gazvoda M, Osmak M, Sarkar B, Kosmrlj J. Chem.-Eur. J. 2014; 20:17296–17299. [PubMed: 25376425]
9. Sava G, Zorzet S, Turrin C, Vita F, Soranzo M, Zabucchi G, Cocchietto M, Bergamo A, DiGiovine S, Pezzoni G, Sartor L, Garbisa S. Clin. Cancer Res. 2003; 9:1898–1905. [PubMed: 12738748]
10. Hartinger CG, Jakupec MA, Zorbas-Seifried S, Groessl M, Egger A, Berger W, Zorbas H, Dyson PJ, Keppler BK. Chem. Biodivers. 2008; 5:2140–2155. [PubMed: 18972504]
11. Trondl R, Heffeter P, Kowol CR, Jakupec MA, Berger W, Keppler BK. Chem. Sci. 2014; 5:2925–2932.Kuhn PS, Pichler V, Roller A, Hejl M, Jakupec MA, Kandioller W, Keppler BK. Dalton Trans. 2015; 44:659–668. [PubMed: 25385191]
12. Aird RE, Cummings J, Ritchie AA, Muir M, Morris RE, Chen H, Sadler PJ, Jodrell DI. Br. J. Cancer. 2002; 86:1652–1657. [PubMed: 12085218] Bergamo A, Masi A, Peacock AFA, Habtemariam A, Sadler PJ, Sava G. J. Inorg. Biochem. 2010; 104:79–86. [PubMed: 19906432]
13. Scolaro C, Bergamo A, Brescacin L, Delfino R, Cocchietto M, Laurenczy G, Geldbach TJ, Sava G, Dyson PJ. J. Med. Chem. 2005; 48:4161–4171. [PubMed: 15943488]
14. Weiss A, Berndsen RH, Dubois M, Müller C, Schibli R, Griffioen AW, Dyson PJ, Nowak-Sliwinska P. Chem. Sci. 2014; 5:4742–4748.
15. Bergamo A, Masi A, Dyson PJ, Sava G. Int. J. Oncol. 2008; 33:1281–1289. [PubMed: 19020762]
16. Nowak-Sliwinska P, van Beijnum JR, Casini A, Nazarov AA, Wagnieres G, van den Bergh H, Dyson PJ, Griffioen AW. J. Med. Chem. 2011; 54:3895–3902. [PubMed: 21534534]
17. Sava G, Jaouen G, Hillard EA, Bergamo A. Dalton Trans. 2012; 41:8226–8234. [PubMed: 22614531]
18. Adhireksan Z, Davey GE, Campomanes P, Groessl M, Clavel CM, Yu HJ, Nazarov AA, Yeo CHF, Ang WH, Droge P, Rothlisberger U, Dyson PJ, Davey CA. Nat. Commun. 2014; 5:3462. [PubMed: 24637564]
19. Dyson PJ, Sava G. Dalton Trans. 2006:1929–1933. [PubMed: 16609762] Guidi F, Modesti A, Landini I, Nobili S, Mini E, Bini L, Puglia M, Casini A, Dyson PJ, Gabbiani C, Messori L. J. Inorg. Biochem. 2013; 118:94–99. [PubMed: 23142974]
20. Barry NPE, Sadler PJ. Chem. Commun. 2013; 49:5106–5131.Kilpin KJ, Dyson PJ. Chem. Sci. 2013; 4:1410–1419.

21. Chen HM, Parkinson JA, Morris RE, Sadler PJ. J. Am. Chem. Soc. 2003; 125:173–186. [PubMed: 12515520]
22. Xie P, Streu C, Qin J, Bregman H, Pagano N, Meggers E, Marmorstein R. Biochemistry. 2009; 48:5187–5198. [PubMed: 19371126] Das S, Sinha S, Britto R, Somasundaram K, Samuelson AG. J. Inorg. Biochem. 2010; 104:93–104. [PubMed: 19913918]
23. Bhat SS, Kumbhar AS, Lonnecke P, Hey-Hawkins E. Inorg. Chem. 2010; 49:4843–4853. [PubMed: 20459107]
24. Kukushkin VY, Pombeiro AJL. Coord. Chem. Rev. 1999; 181:147–175. and references therein.
25. Colak AT, Irez G, Mutlu H, Hokelek T, Caylak N. J. Coord. Chem. 2009; 62:1005–1014.
26. Scaffidi-Domianello YY, Meelich K, Jakupec MA, Arion VB, Kukushkin VY, Galanski M, Keppler BK. Inorg. Chem. 2010; 49:5669–5678. [PubMed: 20459062]
27. Bartel C, Bytzek AK, Scaffidi-Domianello YY, Grabmann G, Jakupec MA, Hartinger CG, Galanski M, Keppler BK. J. Biol. Inorg. Chem. 2012; 17:465–474. [PubMed: 22227950]
28. Ossipov K, Scaffidi-Domianello YY, Seregina IF, Galanski M, Keppler BK, Timerbaev AR, Bolshov MA. J. Inorg. Biochem. 2014; 137:40–45. [PubMed: 24803025]
29. Wirth S, Rohbogner CJ, Cieslak M, Kazmierczak-Baranska J, Donevski S, Nawrot B, Lorenz IP. J. Biol. Inorg. Chem. 2010; 15:429–440. [PubMed: 20091072]
30. Chitrapriya N, Mahalingam V, Zeller M, Lee H, Natarajan K. J. Mol. Struct. 2010; 984:30–38.
31. Chitrapriya N, Mahalingam V, Channels LC, Zeller M, Fronczek FR, Natarajan K. Inorg. Chim. Acta. 2008; 361:2841–2850.
32. Mendoza-Ferri MG, Hartinger CG, Eichinger RE, Stolyarova N, Severin K, Jakupec MA, Nazarov AA, Keppler BK. Organometallics. 2008; 27:2405–2407.
33. Atilla-Gokcumen GE, Di Costanzo L, Meggers E. J. Biol. Inorg. Chem. 2011; 16:45–50. [PubMed: 20821241] Fu Y, Soni R, Romero MJ, Pizarro AM, Salassa L, Clarkson GJ, Hearn JM, Habtemariam A, Wills M, Sadler PJ. Chem.-Eur. J. 2013; 19:15199–15209. [PubMed: 24114923] Kilpin KJ, Cammack SM, Clavel CM, Dyson PJ. Dalton Trans. 2013; 42:2008–2014. [PubMed: 23187957]
34. Blanck S, Maksimoska J, Baumeister J, Harms K, Marmorstein R, Meggers E. Angew. Chem.-Int. Edit. 2012; 51:5244–5246.
35. Brunner H, Oeschey R, Nuber B. Organometallics. 1996; 15:3616–3624.
36. Ward TR, Schafer O, Daul C, Hofmann P. Organometallics. 1997; 16:3207–3215.
37. Faller JW, Patel BP, Albrizzio MA, Curtis M. Organometallics. 1999; 18:3096–3104.
38. Therrien B, Ward TR. Angew. Chem.-Int. Edit. 1999; 38:405–408.
39. Larionov SV. Russ. J. Coord. Chem. 2012; 38:1–23. and references therein.
40. Chahboun G, Brito JA, Royo B, El Amrani MA, Gomez-Bengoa E, Mosquera MEG, Cuenca T, Royo E. Eur. J. Inorg. Chem. 2012:2940–2949.Zelewsky A. Coord. Chem. Rev. 1999; 190–192:811–825.
41. Brecknell DJ, Carman RM, Singaram B, Verghese J. Aust. J. Chem. 1977; 30:195–203.
42. Ibn El Alami MS, El Amrani MA, Dahdouh A, Roussel P, Suisse I, Mortreux A. Chirality. 2012; 24:675–682. [PubMed: 22711228]
43. Tkachev AV, Rukavishnikov AV, Chibiryaev AM, Denisov AY, Gatilov YV, Bagryanskaya IY. Aust. J. Chem. 1992; 45:1077–1086.
44. Noyori R, Hashiguchi S. Accounts Chem. Res. 1997; 30:97–102.Davenport AJ, Davies DL, Fawcett J, Russell DR. Dalton Trans. 2004:1481–1492. [PubMed: 15252645] Touge T, Hakamata T, Nara H, Kobayashi T, Sayo N, Saito T, Kayaki Y, Ikariya T. J. Am. Chem. Soc. 2011; 133:14960–14963. [PubMed: 21870824]
45. Shabalina IY, Kirin VP, Maksakov VA, Virovets AV, Golovin AV, Agafontsev AM, Tkachev AV. Russ. J. Coord. Chem. 2008; 34:286–294.Kirin VP, Prikhod'ko IY, Maksakov VA, Virovets AV, Agafontsev AM, Golovin BA. Russ. Chem. Bull. 2009; 58:1371–1382.
46. Butenschon H. Chem. Rev. 2000; 100:1527–1564. [PubMed: 11749275]
47. Cabrita EJ, Berger S. Magn. Reson. Chem. 2001; 39:S142–S148.

48. Garcia-Frutos EM, Hennrich G, Gutierrez E, Monge A, Gomez-Lor B. J. Org. Chem. 2010; 75:1070–1076. [PubMed: 20073515] Dossel LF, Kamm V, Howard IA, Laquai F, Pisula W, Feng XL, Li C, Takase M, Kudernac T, De Feyter S, Mullen K. J. Am. Chem. Soc. 2012; 134:5876–5886. [PubMed: 22394147]
49. Baumann SO, Bendova M, Fric H, Puchberger M, Visinescu C, Schubert U. Eur. J. Inorg. Chem. 2009:3333–3340.
50. Singh SK, Sharma S, Dwivedi SD, Zou RQ, Xu Q, Pandey DS. Inorg. Chem. 2008; 47:11942–11949. [PubMed: 19006287]
51. Werner H, Daniel T, Knaup W, Nurnberg O. Journal of Organometallic Chemistry. 1993; 462:309–318.
52. Li YQ, de Kock C, Smith PJ, Chibale K, Smith GS. Organometallics. 2014; 33:4345–4348.
53. Martin RB. Chem. Rev. 2005; 96:3043–3064. [PubMed: 11848852] Kastler M, Pisula W, Wasserfallen D, Pakula T, Mullen K. J. Am. Chem. Soc. 2005; 127:4286–4296. [PubMed: 15783210]
54. All the NMR dilution data fit nicely to the assumptions of both equations derived from the infinite association and dimerization models. Thus, we did not examine the model in which the association constant for dimerization is different from those for the formation of higher aggregates.
55. Ciancaleoni G, Di Maio I, Zuccaccia D, Macchioni A. Organometallics. 2007; 26:489–496. and references therein.
56. Bolano S, Ciancaleoni G, Bravo J, Gonsalvi L, Macchioni A, Peruzzini M. Organometallics. 2008; 27:1649–1652.
57. Zuccaccia D, Macchioni A. Organometallics. 2005; 24:3476–3486.
58. Burini A, Fackler JP, Galassi R, Macchioni A, Omary MA, Rawashdeh-Omary MA, Pietroni BR, Sabatini S, Zuccaccia C. J. Am. Chem. Soc. 2002; 124:4570–4571. [PubMed: 11971698]
59. Tobe Y, Utsumi N, Kawabata K, Nagano A, Adachi K, Araki S, Sonoda M, Hirose K, Naemura K. J. Am. Chem. Soc. 2002; 124:5350–5364. [PubMed: 11996576]
60. Zuccaccia D, Foresti E, Pettirossi S, Sabatino P, Zuccaccia C, Macchioni A. Organometallics. 2007; 26:6099–6105.
61. Varbanov HP, Goschl S, Heffeter P, Theiner S, Roller A, Jensen F, Jakupec MA, Berger W, Galanski M, Keppler BK. J. Med. Chem. 2014; 57:6751–6764. [PubMed: 25032896]
62. Morais TS, Santos FC, Jorge TF, Corte-Real L, Madeira PJA, Marques F, Robalo MP, Matos A, Santos I, Garcia MH. J. Inorg. Biochem. 2014; 130:1–14. [PubMed: 24145065]
63. Takacsnovak K, Avdeef A, Box KJ, Podanyi B, Szasz G. J. Pharm. Biomed. Anal. 1994; 12:1369–1377. [PubMed: 7849133]
64. Scaffidi-Domianello YY, Legin AA, Jakupec MA, Arion VB, Kukushkin VY, Galanski M, Keppler BK. Inorg. Chem. 2011; 50:10673–10681. [PubMed: 21951170]
65. Siegel R, Miller K, Jemal A. CA-Cancer J. Clin. 2015; 65:5–29. [PubMed: 25559415]
66. Oh WK, Tay MH, Huang JT. Cancer. 2007; 109:477–486. [PubMed: 17186531]
67. Saylor PJ. Asian J. Androl. 2014; 16:341–347. [PubMed: 24435057]
68. Gama S, Mendes F, Marques F, Santos IC, Carvalho MF, Correia I, Pessoa JC, Santos I, Paulo A. J. Inorg. Biochem. 2011; 105:637–644. [PubMed: 21450266]
69. Tomaz AI, Jakusch T, Morais TS, Marques F, de Almeida RFM, Mendes F, Enyedy EA, Santos I, Pessoa JC, Kiss T, Garcia MH. J. Inorg. Biochem. 2012; 117:261–269. [PubMed: 22877927]
70. Wei, Y.; Au, JS. Integration/Interaction of Oncologic Growth. Meadows, G., editor. Vol. 15. Netherlands: Springer; 2005. Demoro B, de Almeida RFM, Marques F, Matos CP, Otero L, Pessoa JC, Santos I, Rodriguez A, Moreno V, Lorenzo J, Gambino D, Tomaz AI. Dalton Trans. 2013; 42:7131–7146. [PubMed: 23519281] Ceresa C, Bravin A, Cavaletti G, Pellei M, Santini C. Curr. Med. Chem. 2014; 21:2237–2265. [PubMed: 24533815]
71. Biersack B, Effenberger K, Knauer S, Ocker M, Schobert R. Eur. J. Med. Chem. 2010; 45:4890–4896. [PubMed: 20727621]
72. Dabrowiak, JC. Metals in Medicine. Chichester, UK: John Wiley and Sons, Ltd; 2009.

73. Liu HK, Sadler PJ. Accounts Chem. Res. 2011; 44:349–359.
74. Timerbaev AR, Hartinger CG, Aleksenko SS, Keppler BK. Chem. Rev. 2006; 106:2224–2248. [PubMed: 16771448]
75. Chen HM, Parkinson JA, Parsons S, Coxall RA, Gould RO, Sadler PJ. J. Am. Chem. Soc. 2002; 124:3064–3082. [PubMed: 11902898]
76. Allardyce CS, Dyson PJ, Ellis DJ, Heath SL. Chem. Commun. 2001:1396–1397.Allardyce CS, Dyson PJ, Ellis DJ, Salter PA, Scopelliti R. Journal of Organometallic Chemistry. 2003; 668:35–42.
77. Saglam N, Colak A, Serbest K, Dulger S, Guner S, Karabocek S, Belduz AO. Biometals. 2002; 15:357–365. [PubMed: 12405530]
78. Hambley TW, Ling ECH, O'Mara S, McKeage MJ, Russell PJ. J. Biol. Inorg. Chem. 2000; 5:675–681. [PubMed: 11128994]
79. Fox, KR. Drug-DNA interactions protocols. Methods in Molecular Biology. New York, USA: Humana Press Inc; 1997.
80. Martinez A, Rajapakse CSK, Sanchez-Delgado RA, Varela-Ramirez A, Lema C, Aguilera RJ. J. Inorg. Biochem. 2010; 104:967–977. [PubMed: 20605217]
81. Lacowicz, JR. Principles of Fluorescence Spectroscopy. New York, USA: Kluwer Academy; 1999.
82. Carreira M, Calvo-Sanjuan R, Sanau M, Zhao XB, Magliozzo RS, Marzo I, Contel M. J. Inorg. Biochem. 2012; 116:204–214. [PubMed: 23063789]

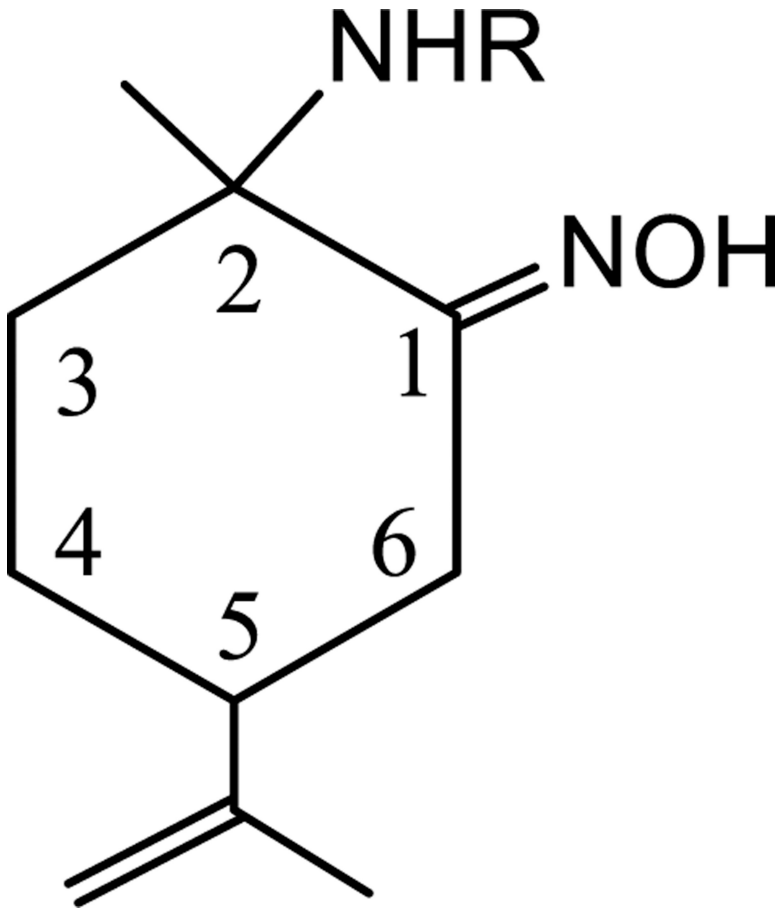

Figure 1.
Numbering of some of the different protons of amino-oxime ligands present in **1a, 1b**

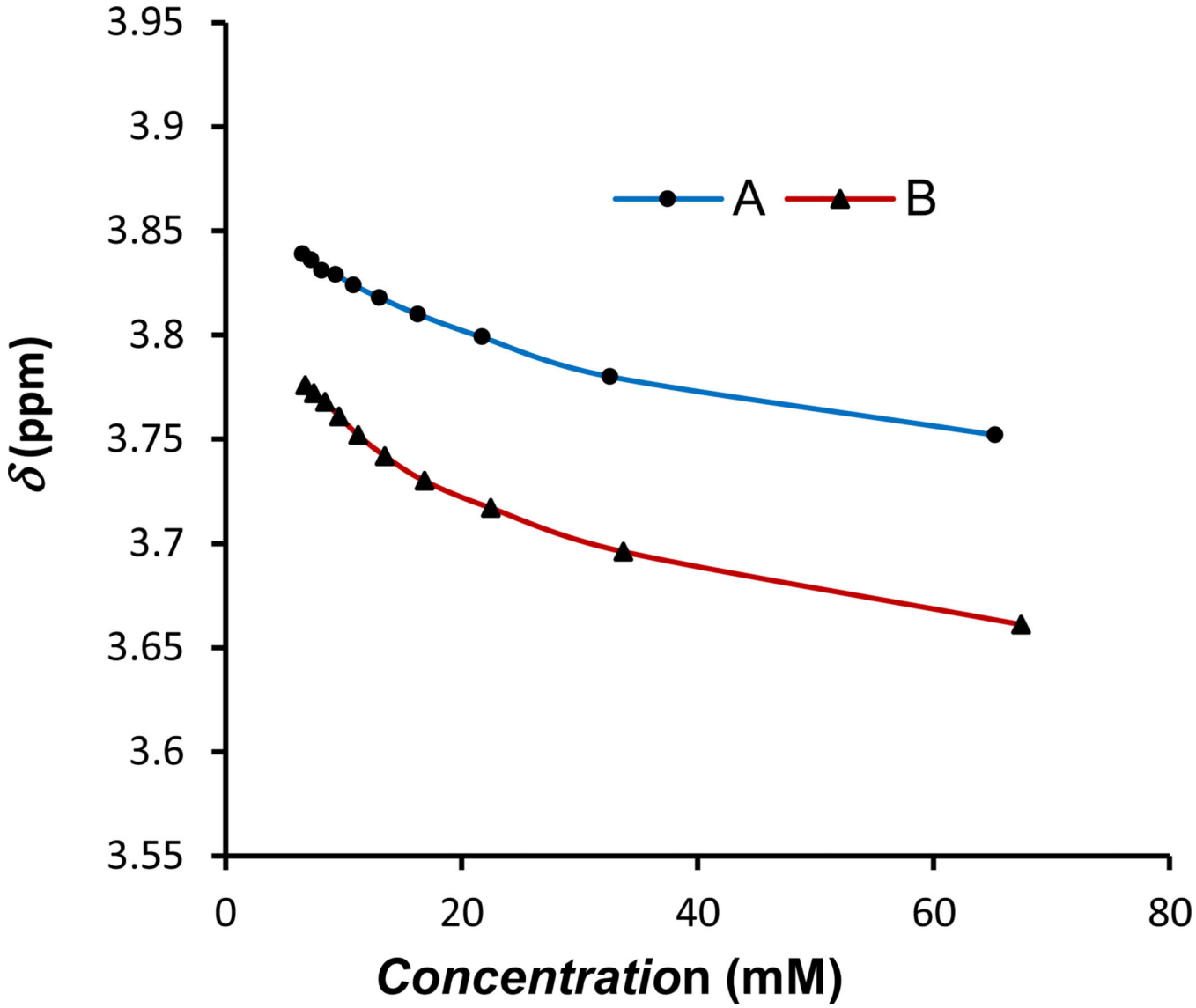

Figure 2.

Concentration dependence of ^{1}H NMR chemical shifts for one of the −CH_2[6] protons of A) compound **1a** in $CDCl_3$, B) compound **1b** in $CDCl_3$.

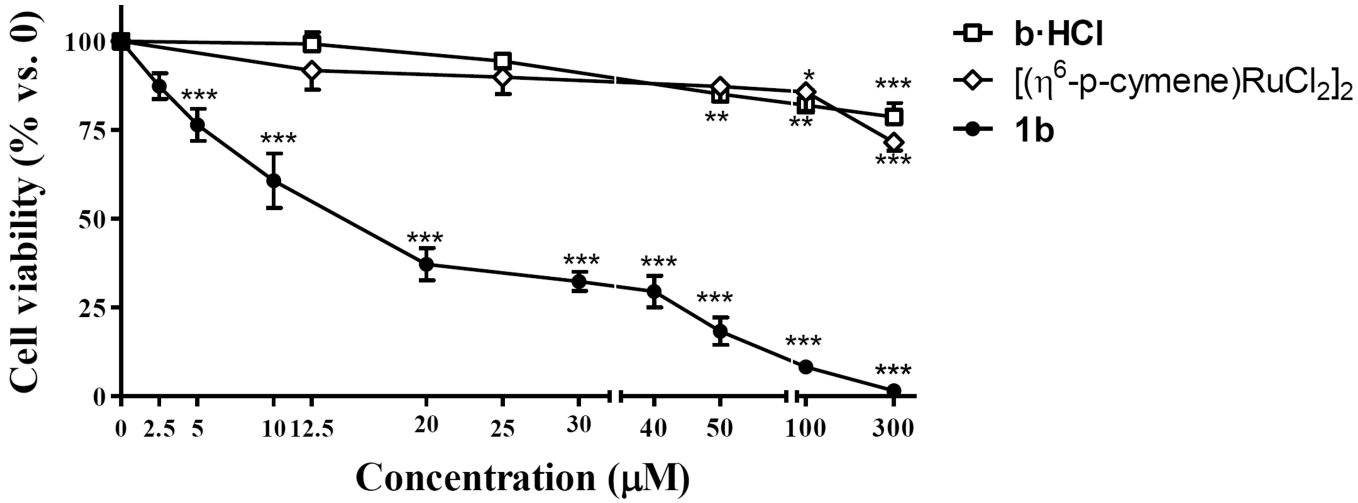

Figure 3.

Effect of derivative **1b** on PC3 cells viability, compared to that of ammonium-oxime compound **b·HCl** and ruthenium dimer $[(\eta^6\text{-}p\text{-cymene})RuCl_2]_2$. Cells were treated with increasing doses of organic and ruthenium compounds for 3 hours. Cell viability was measured by means of MTT assay. The results are expressed as a percentage of live cells compared to control. Data are the mean ± S.E.M. of at least three experiments. *, $P < 0.05$; **, $P < 0.01$; ***, $P < 0.001$ versus Control.

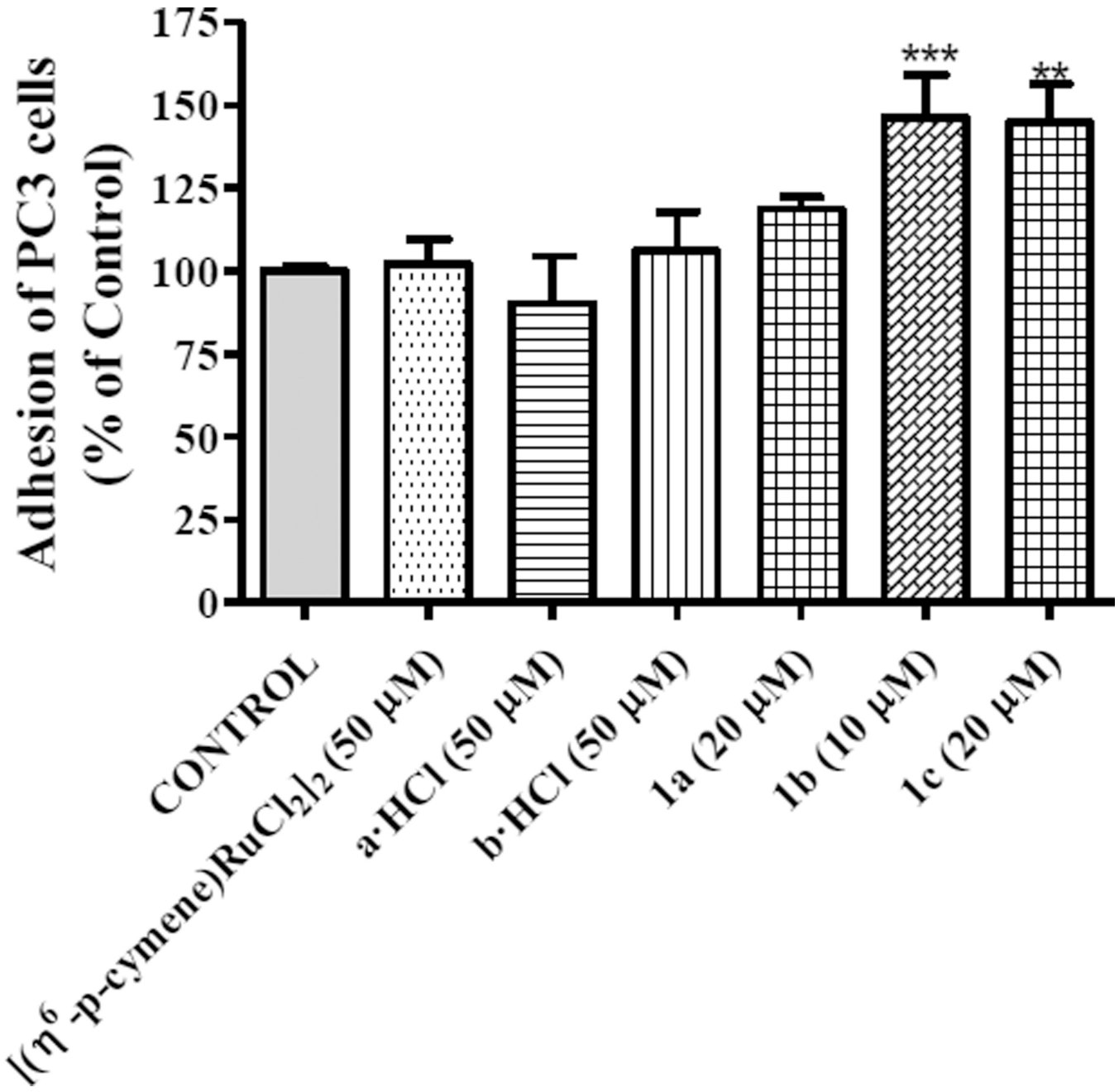

Figure 4.

Effect of **1a-1c** complexes on adhesion of PC3 cells to type-I collagen was studied after treatment with organic and organometallic compounds for 40 min. Data are the mean ± S.E.M. of at least three experiments. **, $P < 0.01$; ***, $P < 0.001$ versus Control.

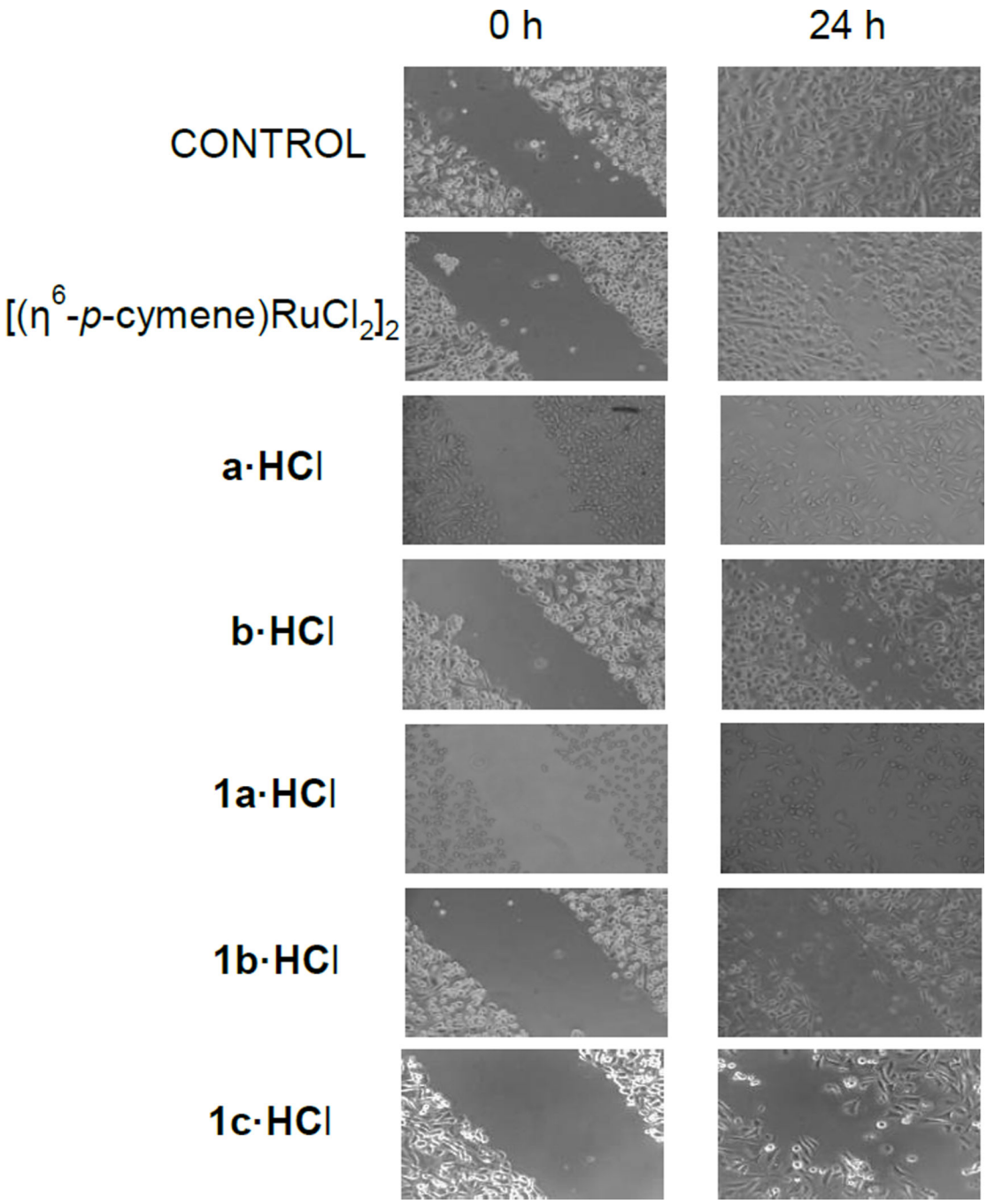

Figure 5.

The effect of organic and organometallic compounds on cell migration was studied in human prostate cancer PC3 cell line. Microscopic analysis of the cell-free area was carried out at the indicated time (24 h) after the addition of the neuropeptide and the width of the area invaded by prostate cells was estimated.

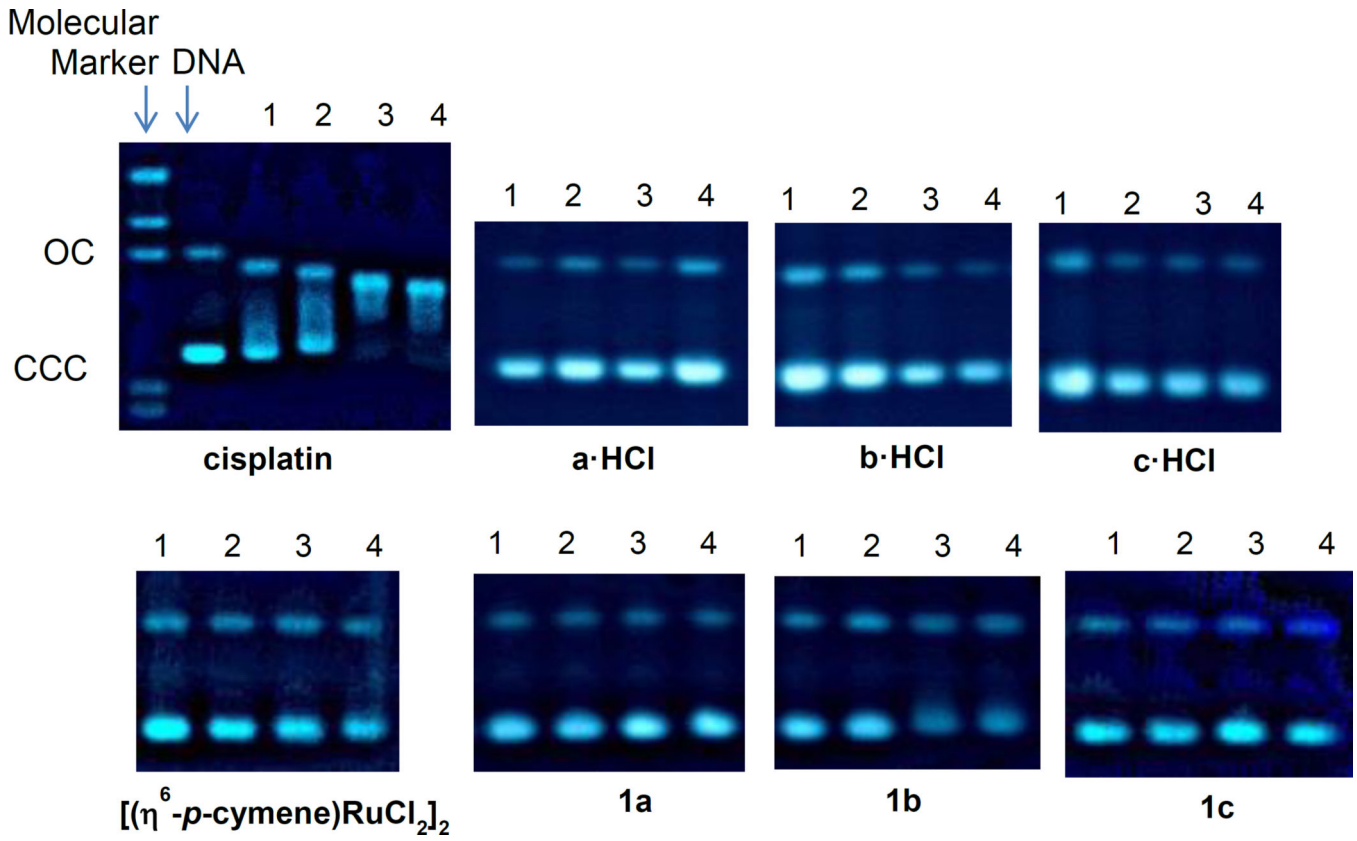

Figure 6.

Electrophoresis mobility shift assays for cisplatin, $[(\eta^6\text{-}p\text{-cymene})RuCl_2]_2$, derivatives **a·HCl-c·HCl** and compounds **1a-1c** (see Experimental for details). DNA refers to untreated plasmid pBR322. 1, 2, 3 and 4 correspond to metal/DNAbp ratios of 0.25, 0.5, 1.0 and 2.0 respectively.

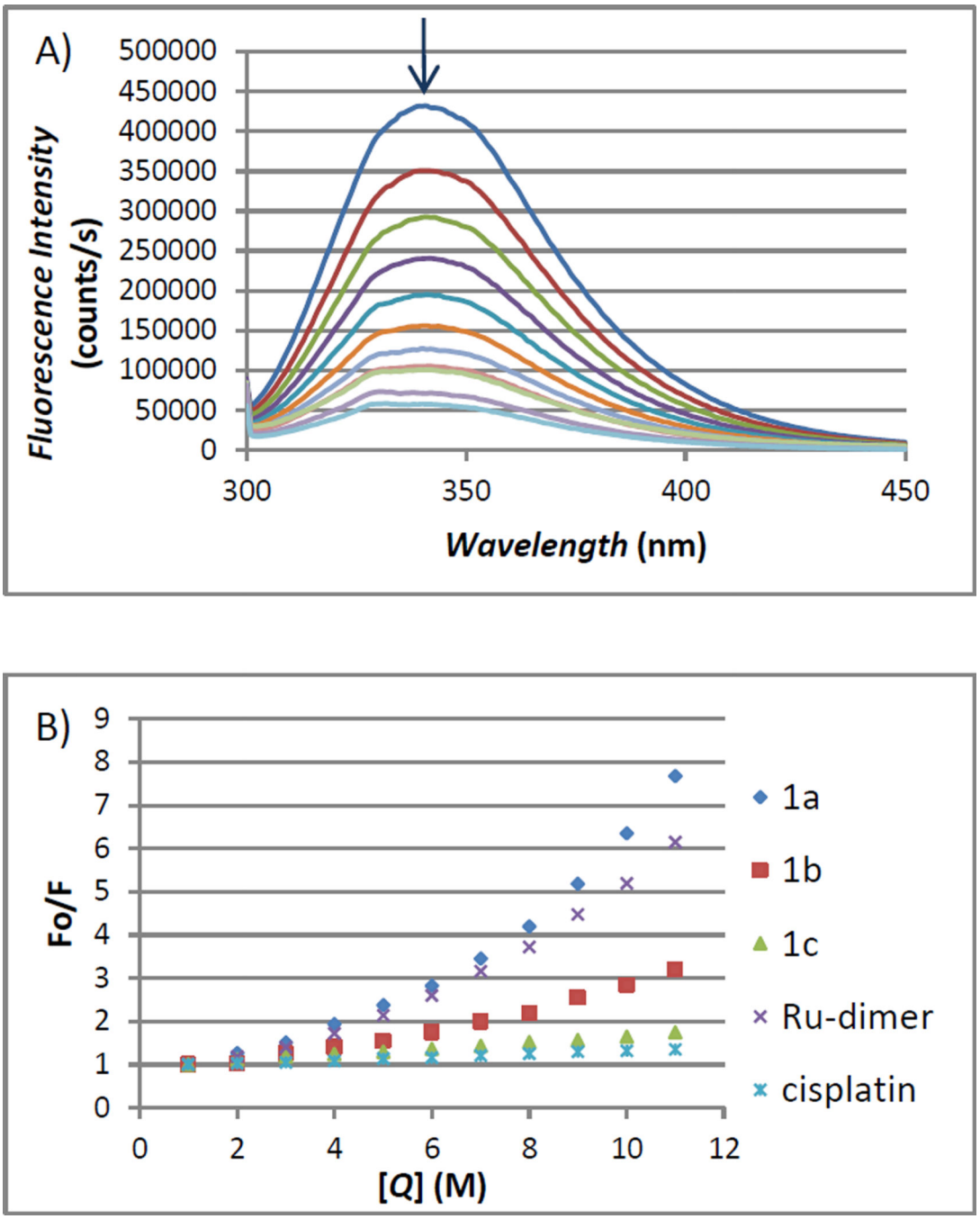

Figure 7.

(A) Fluorescence titration curve of HSA with compound **1a**. Arrow indicates the increase of quencher concentration (10–100 μM). (B) Stern-Volmer plot for HSA fluorescence quenching observed with compounds **1a-1c**, $[(\eta^6\text{-}p\text{-cymene})RuCl_2]_2$ and cisplatin.

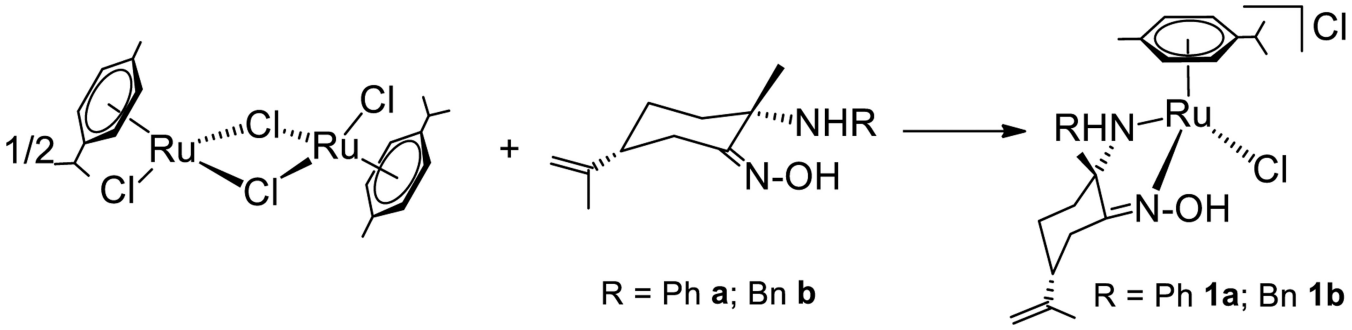

Scheme 1.
Synthesis of chiral amino-oxime ruthenium compounds.

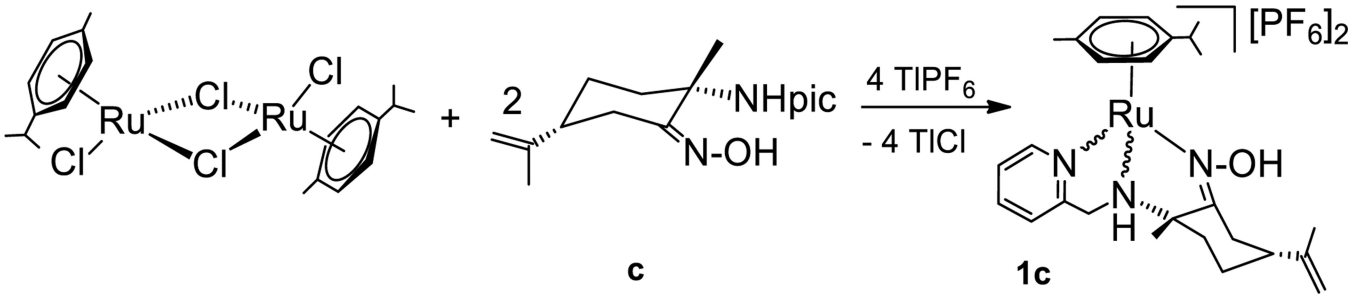

Scheme 2.
Synthesis of picolylamino-oxime ruthenium stereoisomers

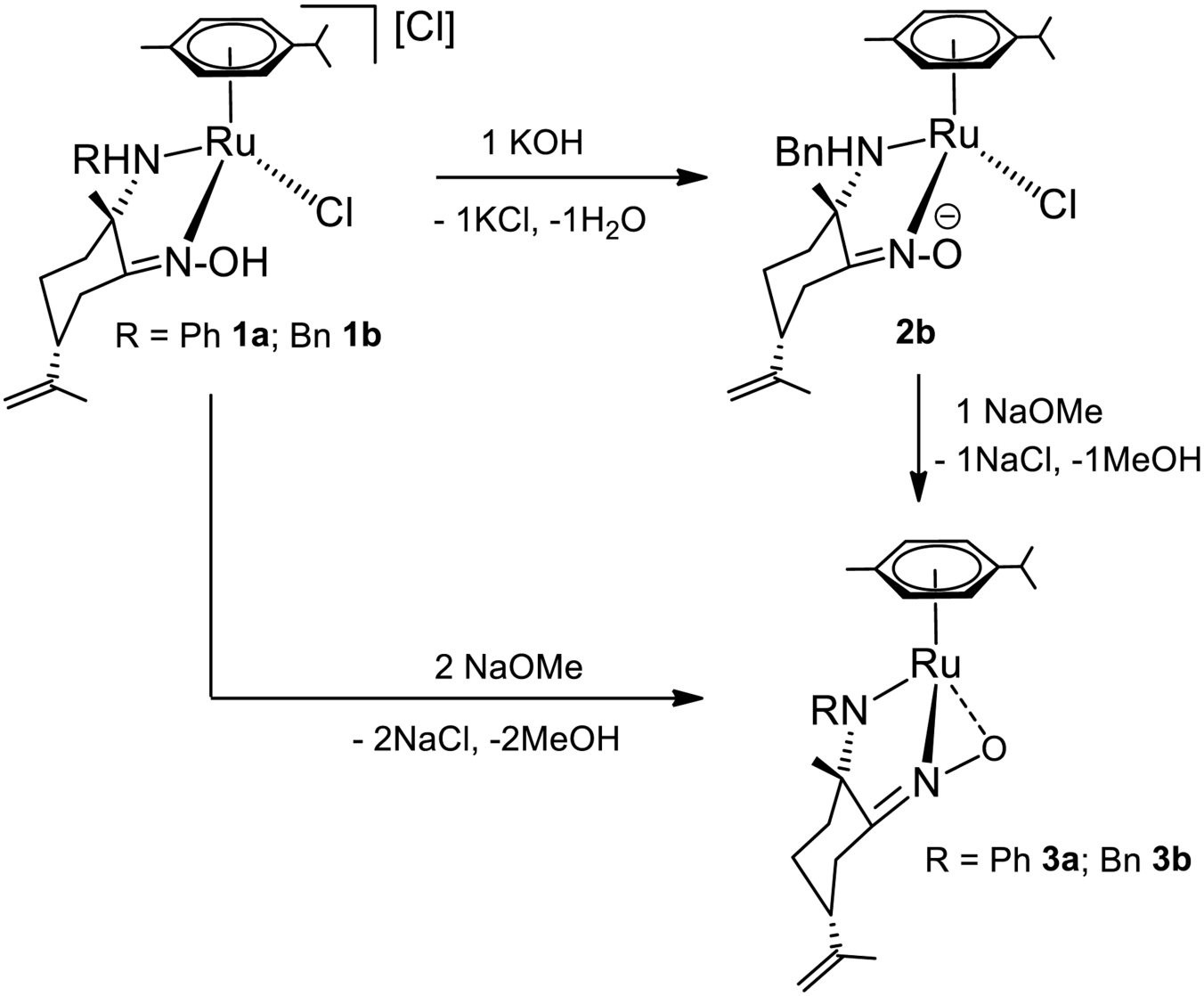

Scheme 3.
Synthesis of amido-oximate ruthenium compounds **3a, 3b**

Table 1

Dimerization Constants and Thermodynamic Parameters for Self-Aggregation of compounds **1a** and **1b** at 295 K.

Compound	Solvent	K_a (M^{-1})	$-\Delta G$ ($Kj \cdot mol^{-1}$)[a]
1a	$CDCl_3$	13.27 ± 1.54	6.34
1b	$CDCl_3$	29.95 ± 3.78	8.34

[a] Calculated by means of equation $\Delta G = -RTlnK$.

Table 2

Diffusion coefficients (D, $m^2 \cdot s^{-1}$) for solutions of TMSS (1mM) and TMSO (1mM) at various concentrations (C, mM) of compounds **1a-c, 2b** and **3b** at 295 K.

Entry	Compound (solvent)	C	$10^{10} \cdot D_s$	D_{TMSS}/D_s	D_{TMSO}/D_{TMSS}	Δr_s
1	**1a** ($CDCl_3$)	11.7	6.957	1.626	0.951	1.00
2	**1a** ($CDCl_3$)	63.0	5.180	2.135	0.955	1.31
3	**1a** ($CDCl_3$:C_6D_6)[a]	5.31	6.685	1.627	0.931	1.00
4	**1a** ($CDCl_3$:C_6D_6)[a]	65.5	3.676	2.889	0.937	1.77
5	**1a** (methanol-d_4)	14.5	6.966	1.385	0.939	1.00
6	**1a** (methanol-d_4)	76.5	6.280	1.475	0.935	1.06
7	**1a** (acetone-d_6)	7.75	11.67	1.584	0.904	1.00
8	**1a** (acetone-d_6)	64.9	10.02	1.704	0.913	1.07
9	**1c** (acetone-d_6)	3.25	10.59	1.852	0.903	1.00
10	**1c** (acetone-d_6)	62.1	10.42	1.882	0.903	1.02
11	**1b** ($CDCl_3$)	6.92	7.894	1.599	0.930	1.19
12	**1b** ($CDCl_3$)	30.7	4.442	2.413	0.945	1.79
13	**1b** ($CDCl_3$)	62.5	3.362	3.147	0.931	2.34
14	**1b·PF$_6$** ($CDCl_3$)	6.93	5.473	1.957	0.949	1.45
15	**1b·PF$_6$** ($CDCl_3$)	52.3	4.346	2.444	0.948	1.82
16	**2b** ($CDCl_3$)	7.38	5.739	1.922	0.948	1.43
17	**2b** ($CDCl_3$)	81.2	4.830	2.284	0.931	1.70
18	**3b** ($CDCl_3$)	5.82	8.542	1.345	0.928	1.00
19	**3b** ($CDCl_3$)	87.1	7.341	1.453	0.929	1.08

[a] $CDCl_3$:C_6D_6 = 8:2

Table 3

IC_{50} (μM) ± S.E.M.[a] for compounds **1a-1c, b·HCl** and $[(\eta^6\text{-}p\text{-cymene})RuCl_2]_2$ in the PC3 cells.

Complex	IC_{50} (μM) ± S.E.M.[a]
1a	24.4 ± 0.75 (3 h)
1b	14.8 ± 0.40 (3 h)
	8.70 ± 1.50 (24 h)
	9.40 ± 4.50 (72 h)
1c	21.5 ± 0.80 (3 h)
b·HCl	177 ± 5.50 (72 h)
$[(\eta^6\text{-}p\text{-cymene})RuCl_2]_2$	213 ± 6.90 (72 h)

[a]Each value represents the mean ± S.E.M. of three independent experiments.

Table 4

Changes in the Tm of CT DNA after incubation with complexes **1a, 1b**, and **1c** for 1h in 5mM tris/$NaClO_4$ buffer at pH 7.39 and r = 0.5.

Complex	ΔT (Tm DNA/Complex-Tm DNA) °C
1a	+ 0.4
1b[a]	---
1c	+ 1.0

[a]Compound **1b** did not afford a single Tm value most plausibly due to its decomposition while heating it in the buffer solution containing DNA.